

Supporting Information

Restricting Shuttling in Bis(imidazolium)...Pillar[5]arene Rotaxanes Using Metal Coordination

Philipp Langer, Lixu Yang, Constance R. Pfeiffer, William Lewis and Neil R. Champness*

Supporting Information Table of Contents

Synthetic Methods	Page 2
Comparison of NMR Spectra	Page 23
Crystallographic Details	Page 27
References	Page 31

1,4-bis-imidazolehexane: 94% ^1H NMR (400 MHz, Chloroform-*d*) δ 7.43 (s, 2H), 7.04 (s, 2H), 6.87 (s, 2H), 3.90 (t, $J = 7.0$ Hz, 4H), 1.76 (d, $J = 7.1$ Hz, 4H), 1.29 (q, $J = 3.8$ Hz, 4H) ppm. ^{13}C NMR (101 MHz, Chloroform-*d*) δ 137.03, 129.53, 118.67, 46.77, 30.85, 26.05. HRMS (ESI+) m/z : 219.1611 ([M+], calc. for $[\text{C}_{12}\text{H}_{19}\text{N}_4]^+$ = 219.1604).

1,4-bis-imidazoleoctane: 90% ^1H NMR (400 MHz, Chloroform-*d*) δ 7.38 (s, 2H), 6.98 (s, 2H), 6.83 (s, 2H), 3.85 (t, $J = 6.3$ Hz, 4H), 1.69 (t, $J = 6.0$ Hz, 4H), 1.26 – 1.16 (m, 8H) ppm. ^{13}C NMR (101 MHz, Chloroform-*d*) δ 136.98, 129.28, 118.72, 46.89, 30.92, 28.80, 26.32. HRMS (ESI+) m/z : 247.1926 ([M+], calc. for $[\text{C}_{14}\text{H}_{23}\text{N}_4]^+$ = 247.1917).

Decamethoxypillar[5]arene

1,4-Dimethoxybenzene (10 g, 72.46 mmol) was added to a flame dried flask which had been backfilled with nitrogen three times. Anhydrous CH_2Cl_2 (500 mL) was added via canula, followed by paraformaldehyde (7 g, 233.34 mmol). The mixture was stirred at room temperature for 10 minutes under a nitrogen atmosphere after which anhydrous iron(III)chloride (2.5 g, 15.43 mmol) was added and the mixture was stirred at room temperature for an additional 3 hours. The mixture was then quenched with water and the organic layer was separated, washed with water and concentrated under reduced pressure. The crude residue was subjected to column chromatography (CH_2Cl_2) to afford the product as a white solid (4.3 g, 40%).

^1H NMR (400 MHz, Chloroform-*d*) δ 6.79 (s, 10H), 3.80 (s, 10H), 3.68 (s, 30H) ppm. ^{13}C NMR (101 MHz, Chloroform-*d*) δ 150.80, 128.24, 114.08, 55.78, 29.67. HRMS (ESI+) m/z : 789.3006 ([M+], calc. for $[\text{C}_{45}\text{H}_{50}\text{O}_{10}\text{K}]^+$ = 789.3041).

2-(iodomethyl)-1,3,5-trimethylbenzene

To a solution of mesitylmethanol (1.88 g, 13 mmol) in dry dioxane (20mL) was added to $\text{BF}_3 \cdot \text{Et}_2\text{O}$ (1.78 g, 13 mmol) and KI (2.08 g, 13 mmol) and the solution was stirred at RT for 4 hours under the exclusion of light. The reaction mixture was poured into ice water and extracted with diethyl ether. The organic layer was washed with brine, dried over anhydrous MgSO_4 and the solvent removed under reduced pressure. The crude product was purified by distillation to give the product as a pale-yellow solid (2.54 g, 75 %).

^1H NMR (400 MHz, Chloroform-*d*) δ 6.87 (s, 2H), 4.50 (s, 2H), 2.36 (s, 6H), 2.29 (s, 3H) ppm. ^{13}C NMR (101 MHz, Chloroform-*d*) δ 137.97, 136.83, 129.42, 21.10, 19.27, 3.96.

General procedure for [2]-Rotaxane 1a-c

Bis-imidazole (0.41 mmol) and pillar[5]arene (0.82 mmol) were dissolved in chloroform (1 mL) and sonicated for 30 minutes. The solution was cooled to -15°C and 2-(iodomethyl)-1,3,5-trimethylbenzene (0.923 mmol) was added under the exclusion of light. The mixture was left to warm to RT and stirred under a nitrogen atmosphere overnight. The crude residue was subjected to column chromatography (Chloroform:methanol 100:2.5) to afford pure **1a-c** as a pale yellow solid

1a 78% ^1H NMR (400 MHz, Chloroform-*d*) δ 8.58 (s, 1H), 8.00 (t, $J = 1.8$ Hz, 2H), 7.04 (s, 4H), 6.83 (s, 10H), 6.63 (t, $J = 1.9$ Hz, 2H), 5.88, 5.98 (ABq, 4H, $J_{\text{AB}} = 16$ Hz), 3.71 (s, 10H), 3.69 (s, 30H), 2.46 (s, 12H), 2.37 (s, 6H), 1.80 – 1.75 (m, 4H), -0.96 – -1.06 (m, 4H) ppm. ^{13}C NMR (101 MHz, Chloroform-*d*) δ 151.14, 140.18, 138.13, 133.53, 130.36, 130.08, 125.79, 123.31, 120.48, 116.02, 77.28, 58.49, 53.47, 49.31, 47.02, 29.16, 23.68, 21.17, 20.24. HRMS (ESI+) m/z : 1205.6625 ([M+], calc. for $[\text{C}_{75}\text{H}_{90}\text{N}_4\text{O}_{10}]^+$ = 1205.6657).

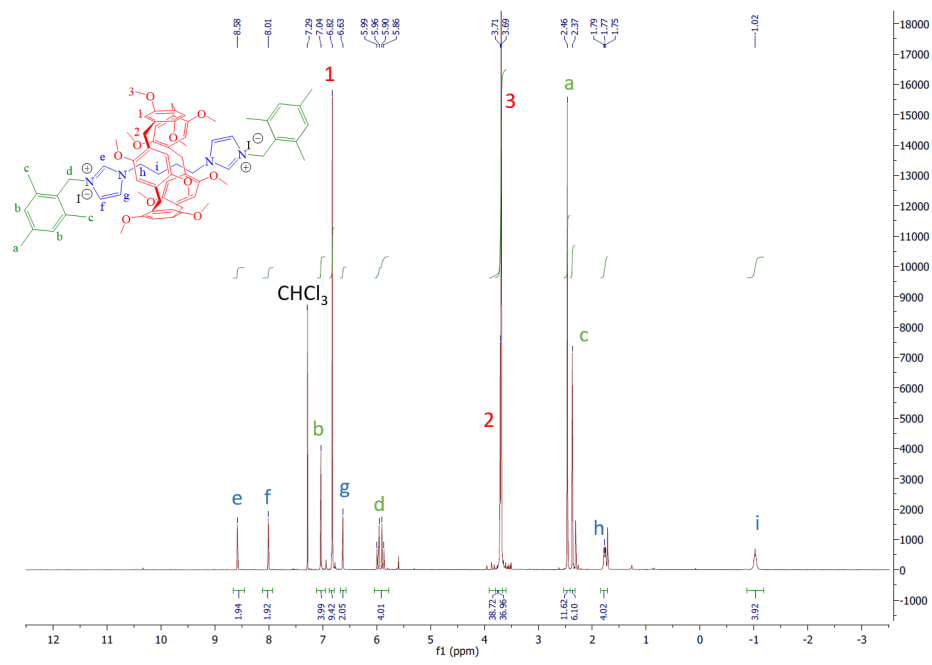


Figure S1. ^1H NMR (400 MHz, CHCl_3 , 298 K) Spectrum of the [2]rotaxane **1a**.

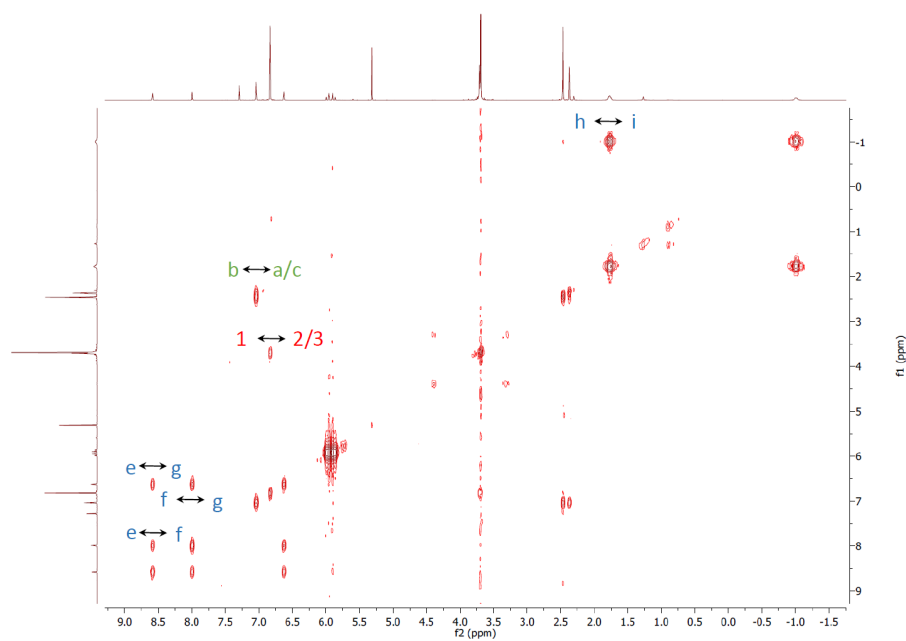


Figure S2. ^1H - ^1H COSY (500 MHz, CHCl_3 , 298 K) spectrum of the [2]rotaxane **1a**.

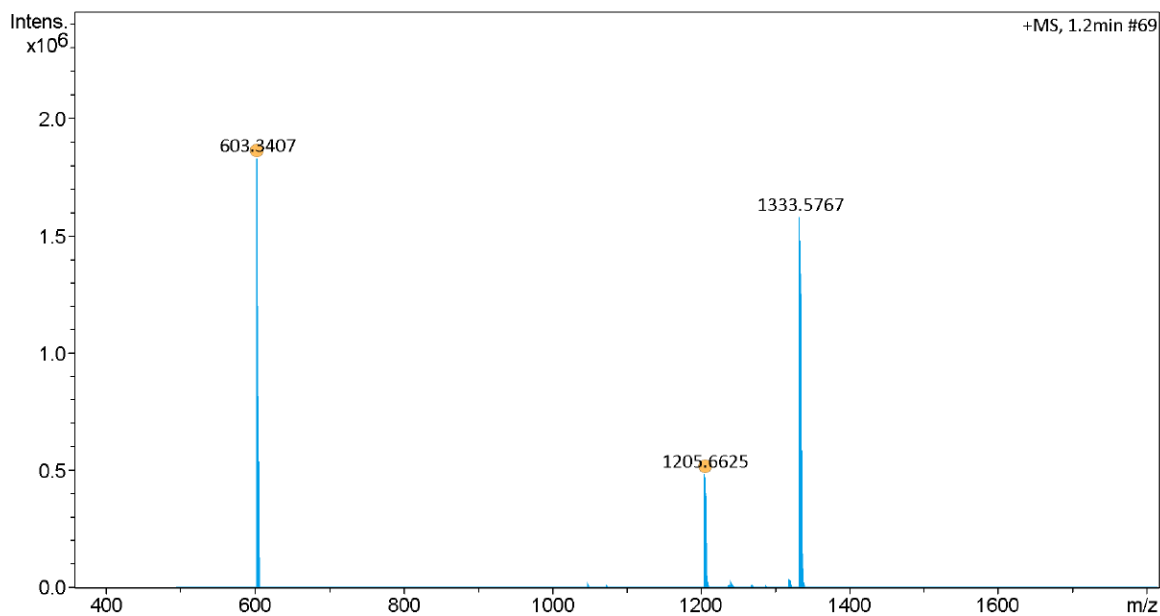


Figure S3. HRMS (ESI positive ionisation mode) of the [2]rotaxane **1a**.

1b 81% ^1H NMR (400 MHz,) δ 8.77 (s, 2H), 6.64 (s, 2H), 7.03 (s, 4H), 6.87 (s, 10H), 6.78 (s, 2H), 5.53, 5.59 (ABq, 4H, $J_{\text{AB}} = 16$ Hz), 3.79 (s, 30H), 3.74 (s, 10H), 2.56 (t, $J = 8.7$ Hz, 4H), 2.40 (s, 12H), 2.38 (s, 6H), 0.45 (s, 4H), 0.31 (s, 4H) ppm. ^{13}C NMR (101 MHz, Chloroform- d) δ 151.16, 140.20, 138.09, 134.47, 130.04, 129.94, 127.88, 122.69, 120.01, 115.80, 58.22, 52.80, 48.02, 29.16, 25.50, 21.13, 20.05, 19.86. HRMS (ESI+) m/z : 1233.6926 ([M^+], calc. for $[\text{C}_{77}\text{H}_{94}\text{N}_4\text{O}_{10}]^+$ = 1233.6970).

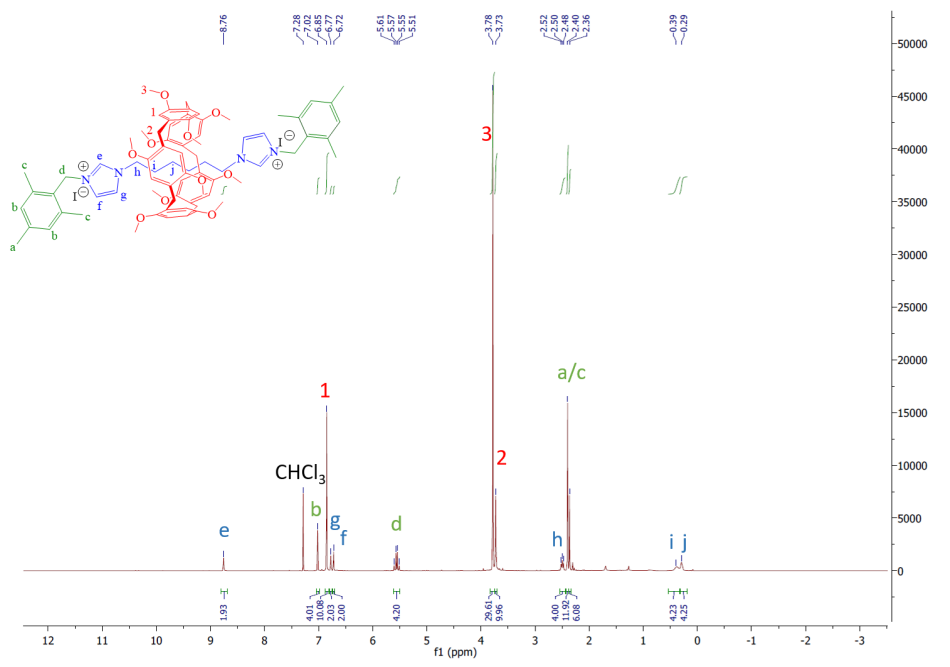


Figure S4. ^1H NMR (400 MHz, CHCl_3 , 298 K) Spectrum of the [2]rotaxane **1b**.

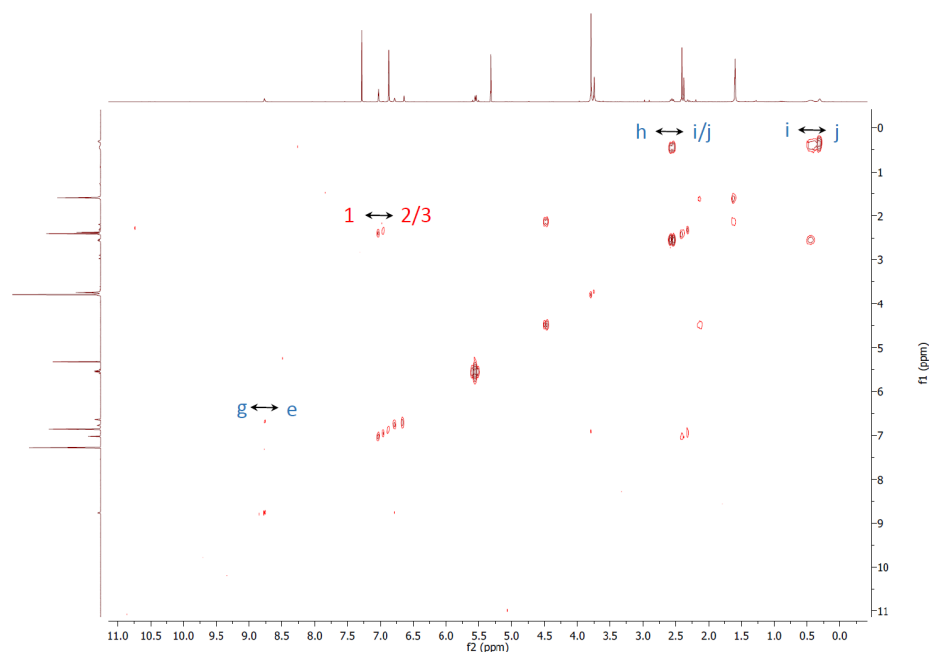


Figure S5. ^1H - ^1H COSY (500 MHz, CHCl_3 , 298 K) spectrum of the [2]rotaxane **1b**.

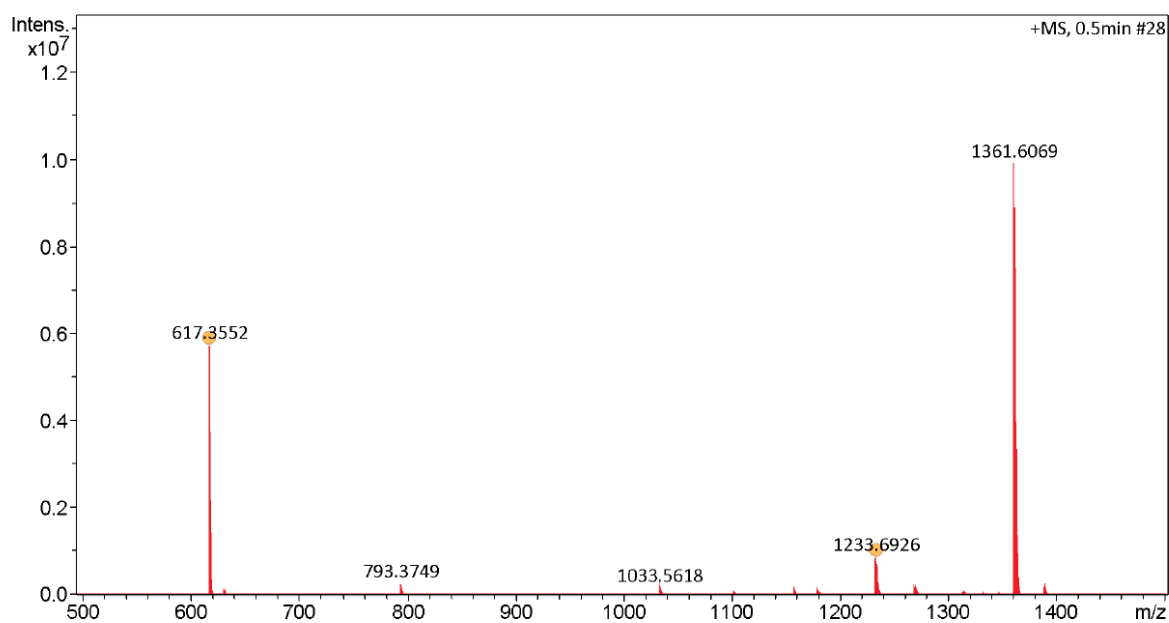


Figure S6. HRMS (ESI positive ionisation mode) of the [2]rotaxane **1b**.

1c 84% ^1H NMR (400 MHz, Chloroform-*d*) δ 7.00 (s, 4H), 6.96 (s, 10H), 6.50 (d, $J = 1.7$ Hz, 2H), 6.37 (d, $J = 1.7$ Hz, 2H), 5.50, 5.58 (ABq, 4H, $J_{\text{AB}} = 16$ Hz), 3.75 (s, 10H), 3.60 (s, 30H), 2.40 (s, 12H), 2.37 (s, 6H), 2.19 – 1.98 (m, 4H), -1.23 – -1.48 (m, 4H) ppm. ^{13}C NMR (101 MHz, Chloroform-*d*) δ 150.95, 140.21, 138.01, 134.32, 130.09, 129.77, 125.12, 122.90, 119.52, 115.37, 77.26, 57.66, 48.54, 47.63, 29.81, 29.10, 28.74, 26.71, 21.13, 19.79. ^1H NMR (400 MHz, DMSO-*d*₆) δ 8.36 (s, 2H), 7.69 (s, 2H), 7.07 (s, 4H), 6.99 (s, 2H), 6.79 (s, 10H), 5.57 – 5.44 (m, 4H), 3.65 (s, 10H), 3.63 (s, 30H), 2.52 – 2.50 (m, 7H), 2.36 (s, 12H), 2.30 (s, 6H), 0.23 – 0.11 (m, 4H), 0.11 – -0.01 (m, 4H), -0.03 – -0.17 (m, 4H). ^{13}C NMR (101 MHz, DMSO-*d*₆) δ 150.54, 139.39, 138.46, 134.43, 130.03, 128.78, 126.91, 122.93, 122.08,

114.32, 56.68, 48.61, 47.77, 29.18, 29.12, 28.31, 26.24, 21.14, 19.76. HRMS (ESI+) m/z: 1261.7263 ([M+], calc. for [C₇₉H₉₈N₄O₁₀]⁺ = 1261.7283).

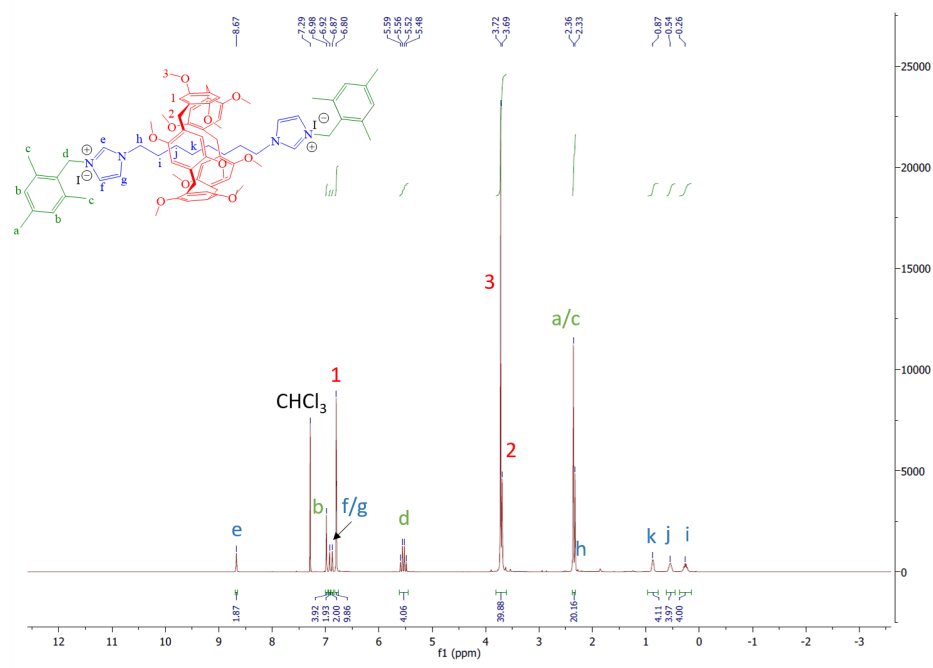


Figure S7. ¹H NMR (400 MHz, CHCl₃, 298 K) Spectrum of the [2]rotaxane **1c**.

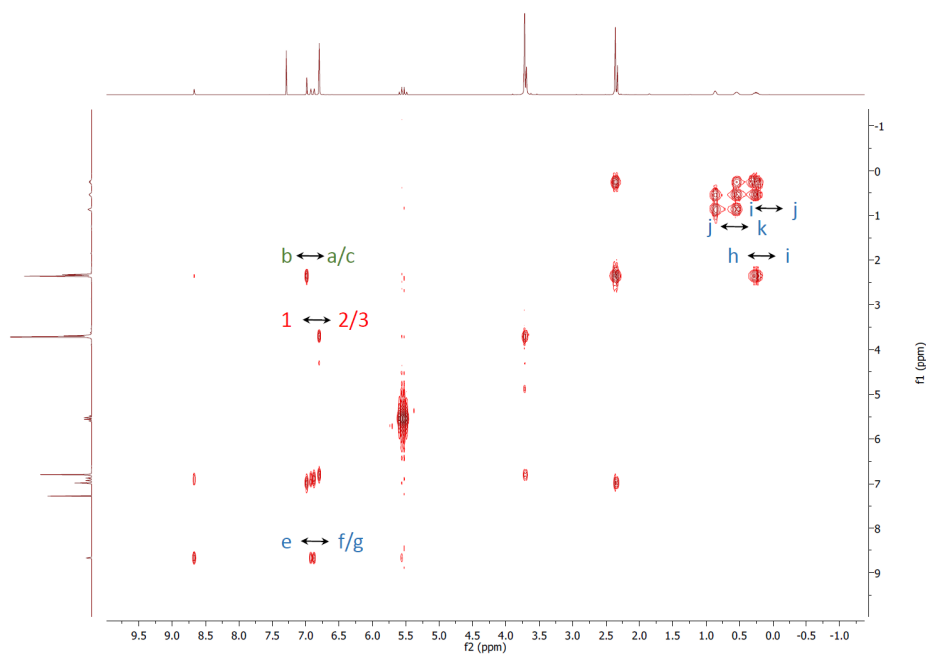


Figure S8. ¹H-¹H COSY (500 MHz, CHCl₃, 298 K) spectrum of the [2]rotaxane **1c**.

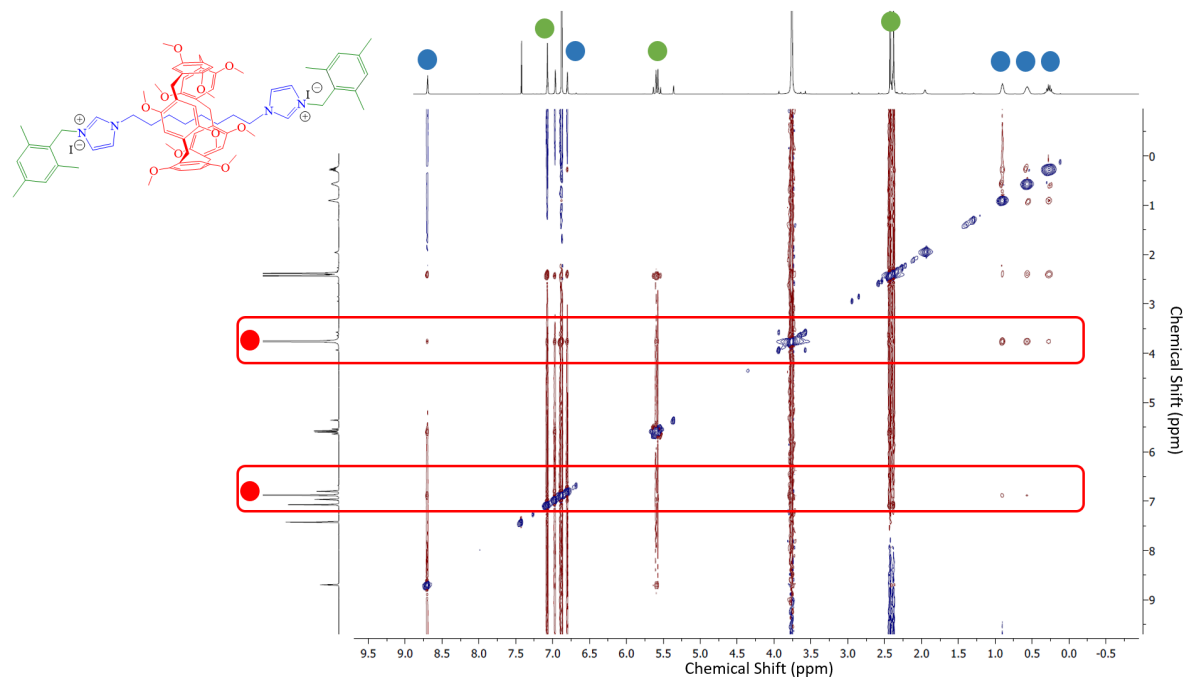


Figure S9. ^1H - ^1H NOESY (400 MHz, CHCl_3 , 298 K) spectrum of the [2]rotaxane **1c**. Showing Pillar[5]arene environments highlighted in red coupling to rod protons shown in blue and green.

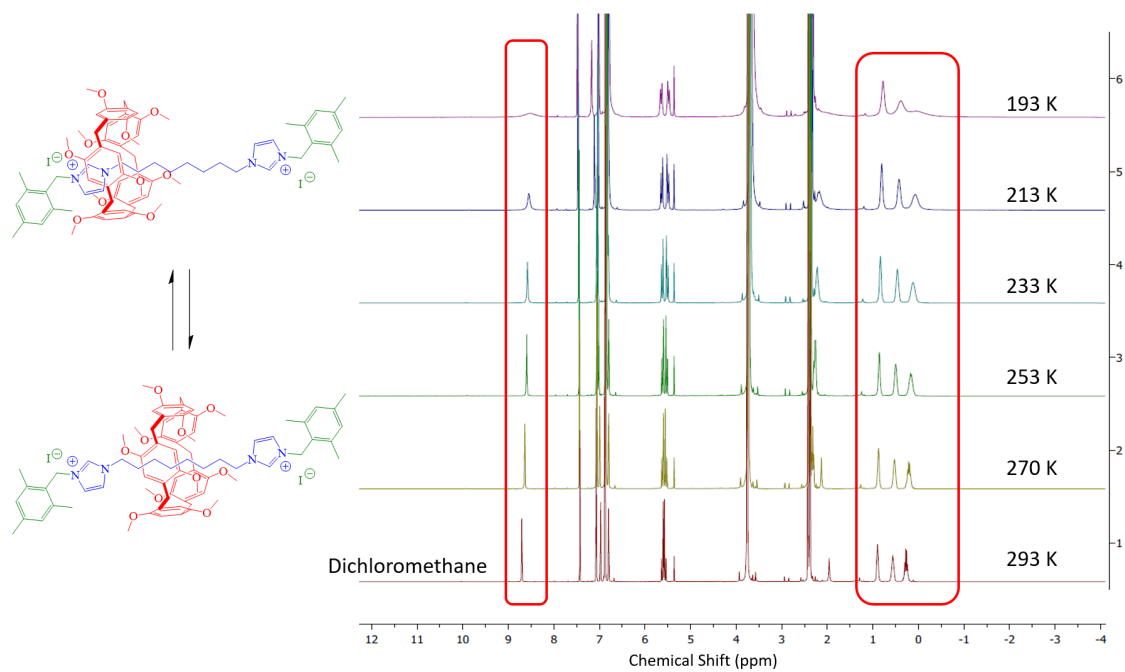


Figure S10. ^1H (400 MHz, CHCl_3 , VT) spectra of the [2]rotaxane **1c**. Showing no change in peak positions therefore indicating that shuttling of the pillar[5]arene is faster than the time scale of the NMR experiment.

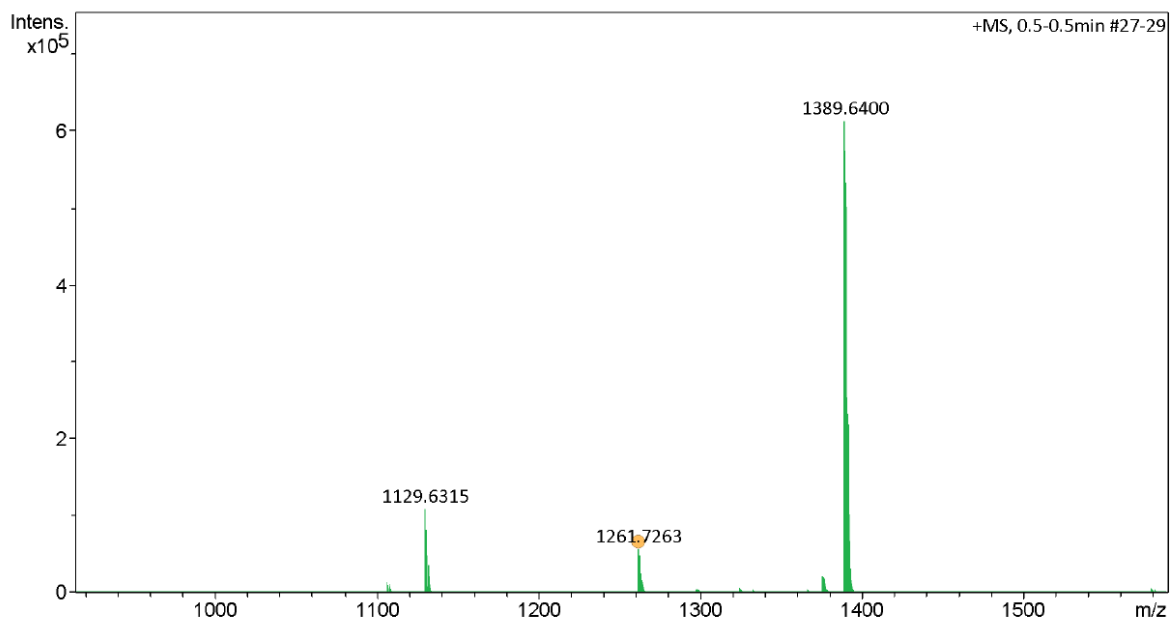


Figure 11. HRMS (ESI positive ionisation mode) of the [2]rotaxane **1c**.

1c (CD₃)₂SO

¹H NMR (400 MHz, DMSO-*d*₆) δ 8.36 (s, 2H), 7.69 (t, *J* = 1.7 Hz, 2H), 7.07 (s, 4H), 6.99 (t, *J* = 1.7 Hz, 2H), 6.79 (s, 10H), 5.56 – 5.45 (m, 4H), 3.65 (s, 10H), 3.63 (s, 30H), 2.51 (m, DMSO+alkane, 10H), 2.36 (s, 12H), 2.30 (s, 6H), 0.16 (s, 4H), 0.05 (p, *J* = 13.9, 7.3 Hz, 4H), -0.09 (s, 4H). ¹³C NMR (101 MHz, DMSO-*d*₆) δ 150.54, 139.39, 138.46, 134.43, 130.03, 128.78, 126.91, 122.93, 122.08, 114.32, 79.68, 56.68, 48.61, 47.77, 29.18, 29.12, 28.31, 26.24, 21.14, 19.76.

1c (CD₃)₂CO

¹H NMR (400 MHz, Acetone-*d*₆) δ 8.71 (s, 2H), 7.60 (t, *J* = 1.8 Hz, 2H), 7.11 (s, 4H), 7.07 (t, *J* = 1.8 Hz, 2H), 6.95 (s, 10H), 5.80 – 5.67 (m, 4H), 3.78 (s, 30H), 3.76 (s, 10H), 2.62 (t, *J* = 8.1 Hz, 4H), 2.47 (s, 12H), 2.35 (s, 6H), 0.72 (s, 4H), 0.40 (s, 4H), 0.33 – 0.19 (m, 4H).

1c NMR Solvent effects comparison

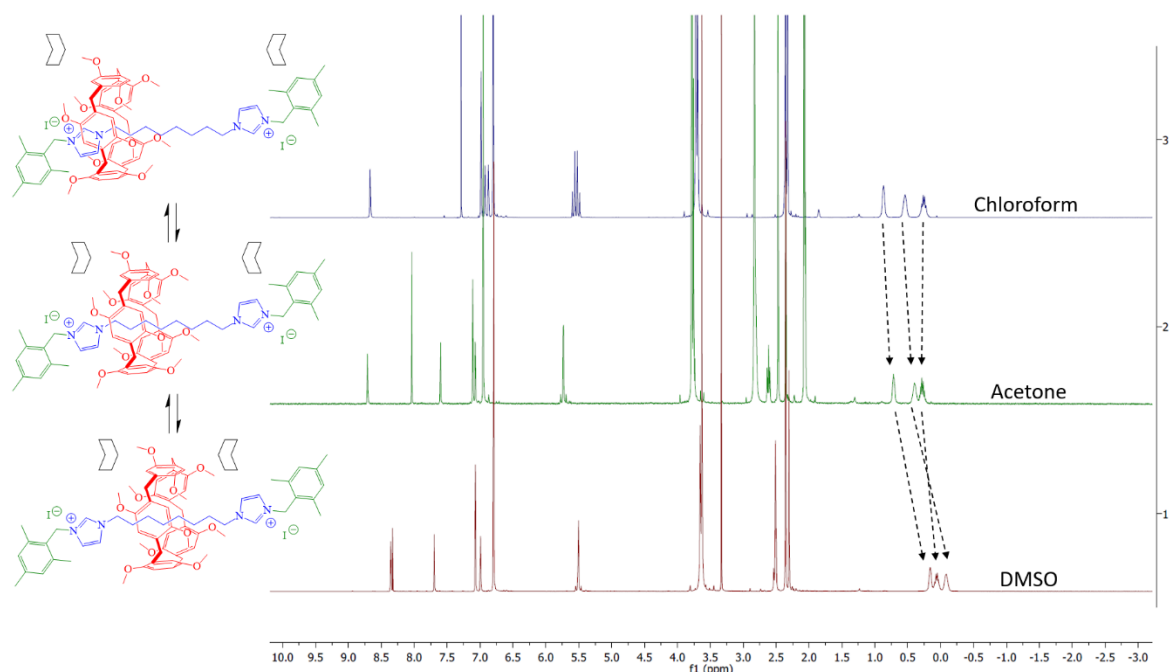


Figure S12. Schematic illustration showing the NMR shifts indicating the pillar[5]arene shuttling range in solvents of increasing polarity.

1c Anion effect (PF₆⁻)

1c (0.1 g, 0.0653 mmol) was dissolved in ethanol (20 mL) and ammonium hexafluorophosphate (0.43 g, 2.61 mmol) was added. The mixture was heated to reflux for 4 hours and left to cool to room temperature. The white precipitate was collected by suction filtration, washed with ethanol and dried to afford the ion exchanged product. ¹H NMR (400 MHz, Chloroform-*d*) δ 7.89 (s, 2H), 7.02 (s, 4H), 6.83 (s, 9H), 6.78 (s, 2H), 6.64 (s, 2H), 5.43 (s, 4H), 3.72 (s, 40H), 2.36 (s, 18H), 2.25 (t, *J* = 8.4 Hz, 4H), 0.84 (s, 4H), 0.51 (s, 4H), 0.35 – 0.00 (m, 4H). ¹³C NMR (101 MHz, Chloroform-*d*) δ 150.87, 140.25, 138.00, 133.78, 130.11, 129.64, 124.95, 122.43, 120.07, 115.13, 57.09, 48.66, 47.51, 29.64, 29.07, 28.31, 26.61, 21.11, 19.44. ¹⁹F NMR (376 MHz, Chloroform-*d*) δ -71.51, -73.41. ³¹P NMR (162 MHz, Chloroform-*d*) δ -130.98, -135.38, -139.78, -144.18, -148.58, -152.97, -157.37.

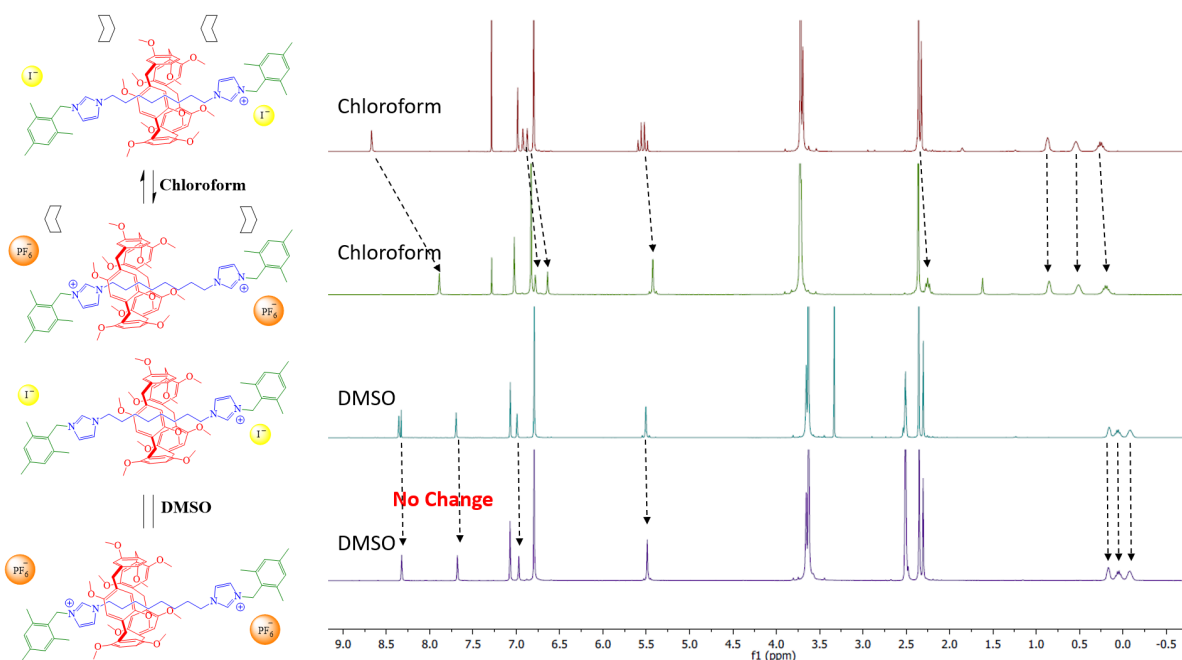


Figure S13. Schematic illustration showing the NMR shifts in **1c** upon anion exchange with ammonium hexafluorophosphate in chloroform and DMSO.

General procedure for Ag-[2]-Rotaxane **2a-c**

To solution of **1a-c** (0.0810 mmol) in CH_2Cl_2 (25 mL) was added Ag_2O (0.0810 mmol) and the mixture was stirred at room temperature overnight under the exclusion of light. The mixture was filtered through a celite plug and the organic fractions were combined, dried over anhydrous MgSO_4 and the solvent removed under reduced pressure to afford the crude product as an off-white powder. This was redissolved in CH_2Cl_2 (1 mL) and added dropwise to cold hexane (20 mL). The white precipitate was collected by filtration under reduced pressure, washed with hexane and dried to afford **2a-c** as white solids.

2a 82% ^1H NMR (400 MHz, Chloroform-*d*) δ 7.01 (s, 4H), 6.91 (s, 10H), 6.64 (d, $J = 1.8$ Hz, 2H), 5.40 (s, 4H), 3.75 (s, 10H), 3.69 (s, 30H), 2.36 (d, $J = 5.8$ Hz, 18H), -0.13 (s, 4H), -2.01 (s, 4H) ppm. ^{13}C NMR (101 MHz, Chloroform-*d*) δ 151.16, 139.02, 137.58, 129.76, 129.73, 115.92, 77.22, 57.76, 50.02, 49.54, 29.12, 23.08, 21.12, 20.11.

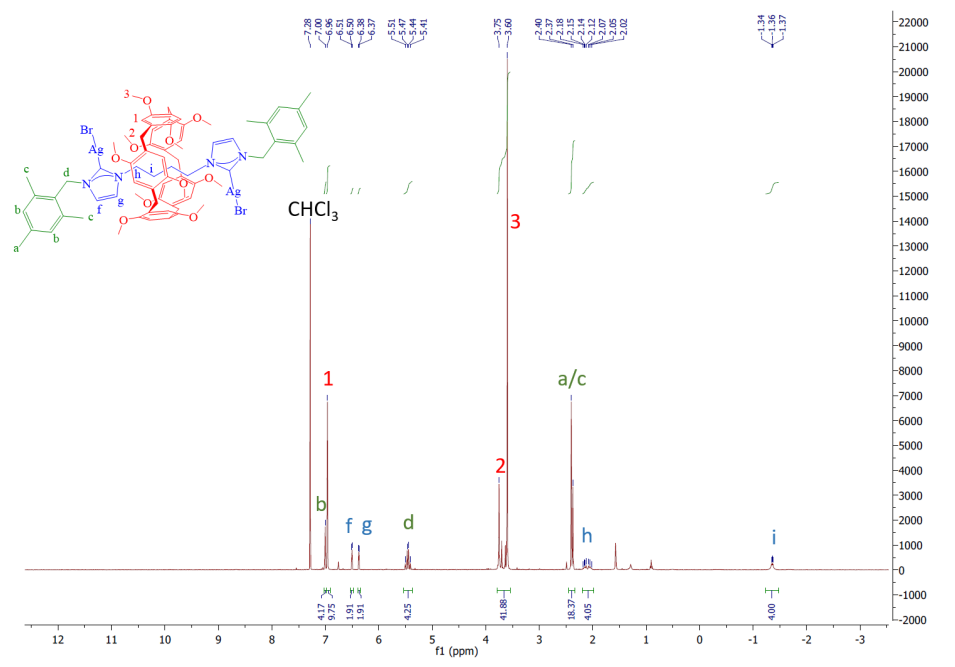


Figure S14. ^1H NMR (400 MHz, CHCl_3 , 298 K) Spectrum of the [2]rotaxane **2a**.

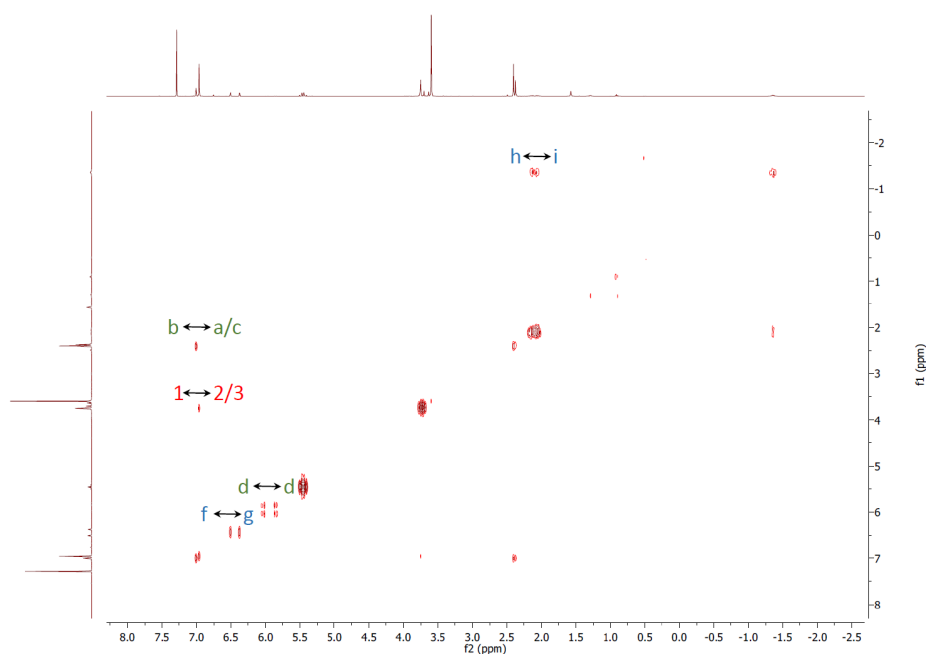


Figure S15. ^1H - ^1H COSY (500 MHz, CHCl_3 , 298 K) spectrum of the [2]rotaxane **2a**.

2b 85% ^1H NMR (400 MHz,) δ 7.28 (d, $J = 1.8$ Hz, 2H), 6.98 (s, 4H), 6.88 (s, 10H), 6.61 (d, $J = 1.8$ Hz, 2H), 5.37 (s, 4H), 3.75 – 3.71 (m, 10H), 3.69 – 3.62 (m, 30H), 3.23 – 3.06 (m, 4H), 2.34 (s, 6H), 2.33 (s, 12H), -0.16 (s, 4H), -2.04 (s, 4H) ppm. ^{13}C NMR (101 MHz, Chloroform- d) δ 150.87, 137.58, 129.87, 129.34, 120.64, 114.93, 57.46, 51.30, 49.68, 29.12, 23.55, 21.12, 19.99.

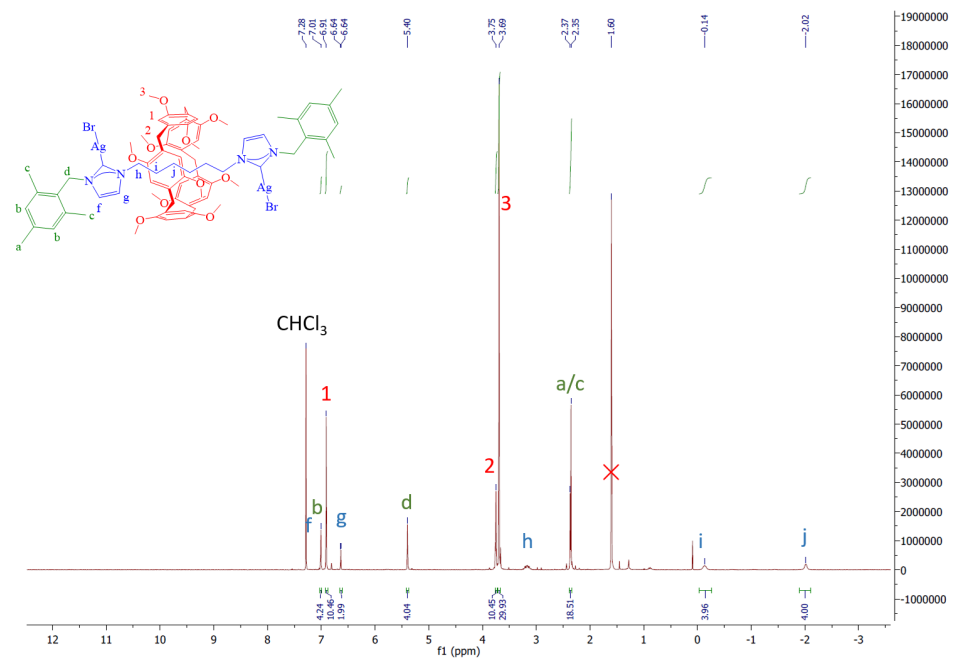


Figure S16. ^1H NMR (400 MHz, CHCl_3 , 298 K) Spectrum of the [2]rotaxane **2b**.

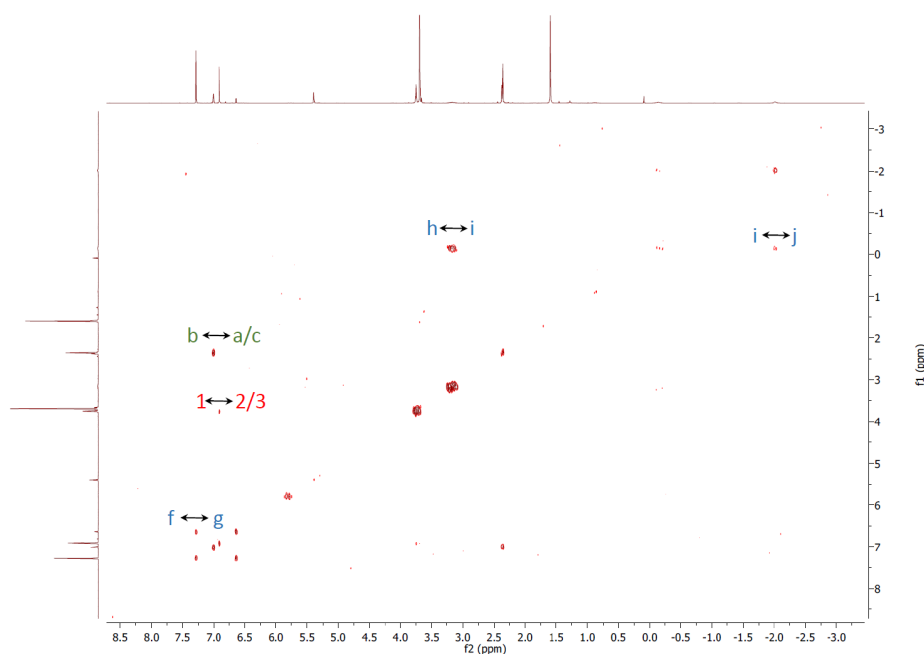


Figure S17. ^1H - ^1H COSY (500 MHz, CHCl_3 , 298 K) spectrum of the [2]rotaxane **2b**.

2c 81% ^1H NMR (400 MHz,) δ 7.19 (d, $J = 1.8$ Hz, 2H), 6.98 (s, 4H), 6.86 (s, 10H), 6.62 (d, $J = 1.9$ Hz, 2H), 5.34 (s, 4H), 3.74 (s, 10H), 3.69 (s, 30H), 3.63 – 3.57 (m, 4H), 2.33 (s, 6H), 2.32 (s, 12H), 0.78 – 0.63 (m, 4H), -0.73 (s, 4H), -1.59 (s, 4H) ppm. ^{13}C NMR (101 MHz, Chloroform- d) δ 150.77, 137.66, 129.84, 128.98, 114.65, 56.84, 52.41, 49.71, 29.13, 25.62, 21.09, 19.96.

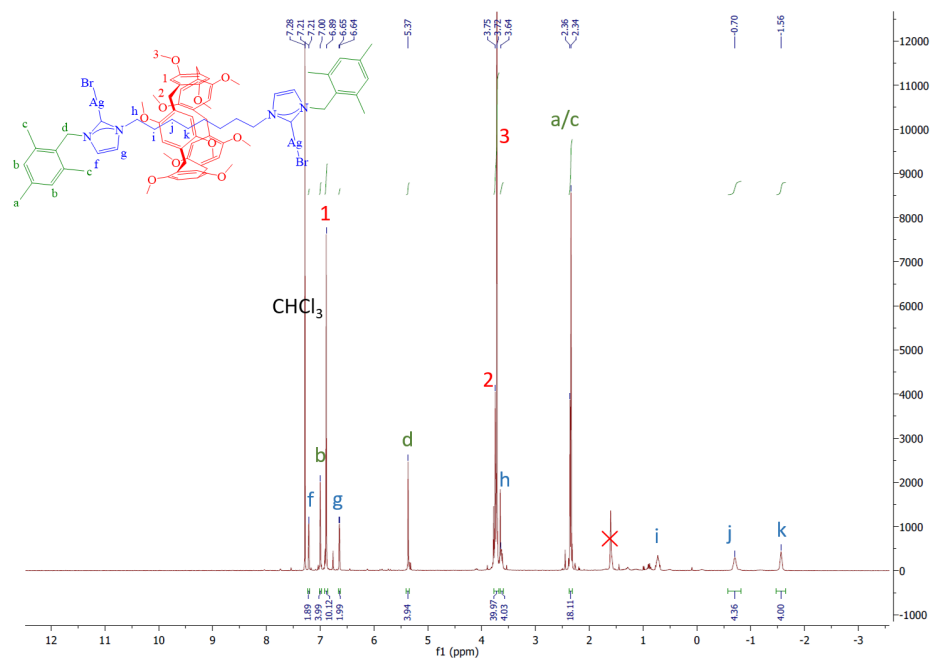


Figure S18. ^1H NMR (400 MHz, CHCl_3 , 298 K) Spectrum of the [2]rotaxane **2c**.

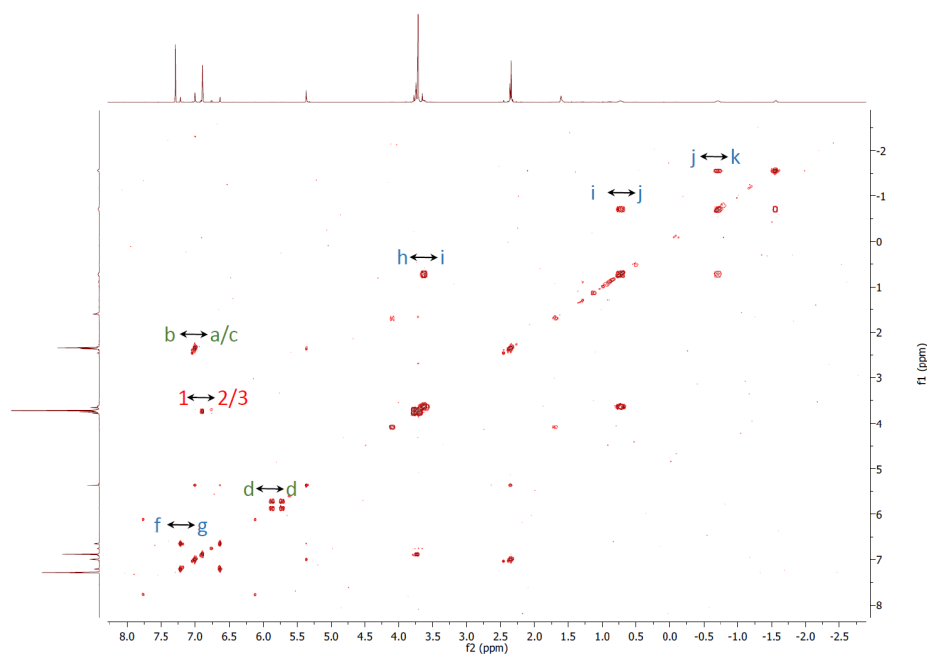


Figure S19. ^1H - ^1H COSY (500 MHz, CHCl_3 , 298 K) spectrum of the [2]rotaxane **2c**.

General Procedure for conversion of rotaxanes **2a-c** to **3a-c**

2a-c (0.062mmol) was added to a flame dried flask which had been backfilled with nitrogen three times. Anhydrous pyridine (10 mL) was added via canula, followed by $\text{Pd}(\text{CH}_3\text{CN})_2\text{Cl}_2$ (0.130mmol) and KI (0.262mmol). The mixture was heated to reflux and stirred overnight under a nitrogen atmosphere and under the exclusion of light. All volatiles were evaporated under reduced pressure and the residue was redissolved in chloroform and water. The organic layer was separated and washed with water, 5% CuSO_4 aq. and brine and subsequently dried over MgSO_4 and filtered. The

solvent was removed under reduced pressure and the residue subjected to a silica pad (CH₂Cl₂) to afford **3a**, **3b** (76 %) and **3c** (69%) as orange powders.

3a 90% ¹H NMR (500 MHz, Chloroform-*d*) δ 7.21 (d, *J* = 2.0 Hz, 1H), 7.09 (s, 2H), 7.06 (s, 5H), 6.96 (s, 2H), 6.71 (s, 5H), 6.33 (d, *J* = 2.0 Hz, 1H), 6.01 (s, 1H), 5.68 (s, 2H), 5.53 (s, 1H), 5.24, 5.43 (ABq, 2H, *J*_{AB} = 10 Hz), 3.96, 4.44 (ABtd, 2H, *J*_{AB} = 240, 5 Hz), 3.98 – 3.64 (m, 40H), 2.49 (s, 6H), 2.41 (s, 3H), 2.37 (s, 7H), 2.35 (s, 4H), 1.07, 1.43 (ABm, 2H, *J*_{AB} = 180 Hz), 0.59, 0.72 (ABtd, 2H, *J*_{AB} = 65, 5 Hz), -0.37, -0.60 (ABm, 2H, *J*_{AB} = 115 Hz). ¹³C NMR-sample was not sufficiently soluble to obtain good quality data. MALDI-TOF M/S *m/z* calcd. for C₇₅H₉₀N₄O₁₀l₂Pd+ [M⁺]: 1565.372, found: 1565.366 (M⁺, C₇₅H₉₀N₄O₁₀l₂Pd, major product).

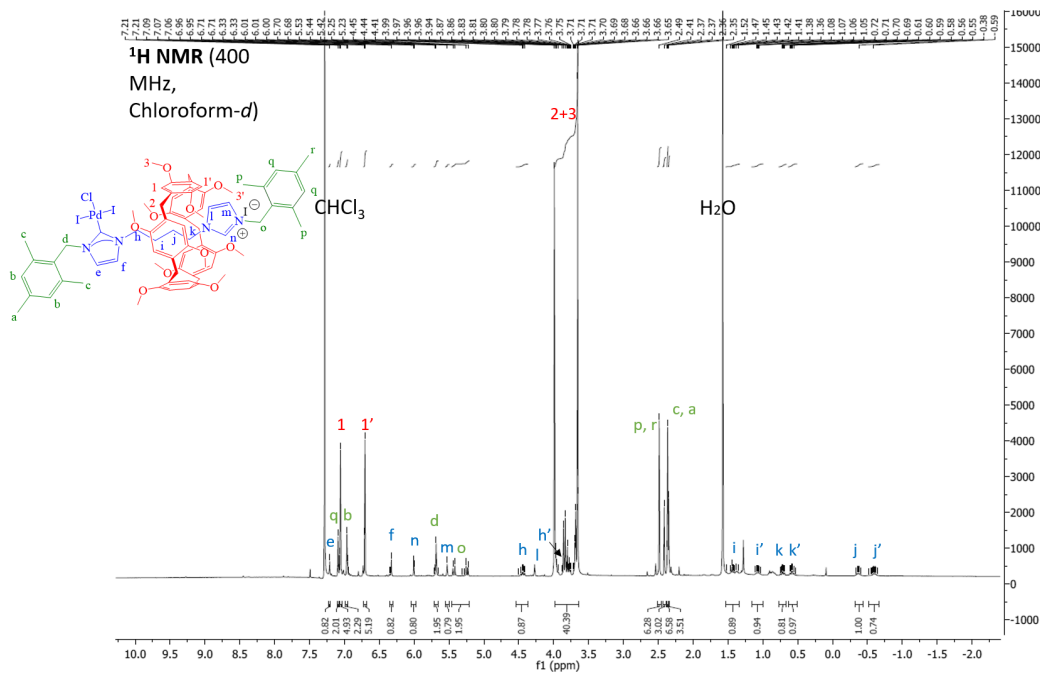


Figure S20. ¹H NMR (400 MHz, CHCl₃, 298 K) Spectrum of the [2]rotaxane **3a**.

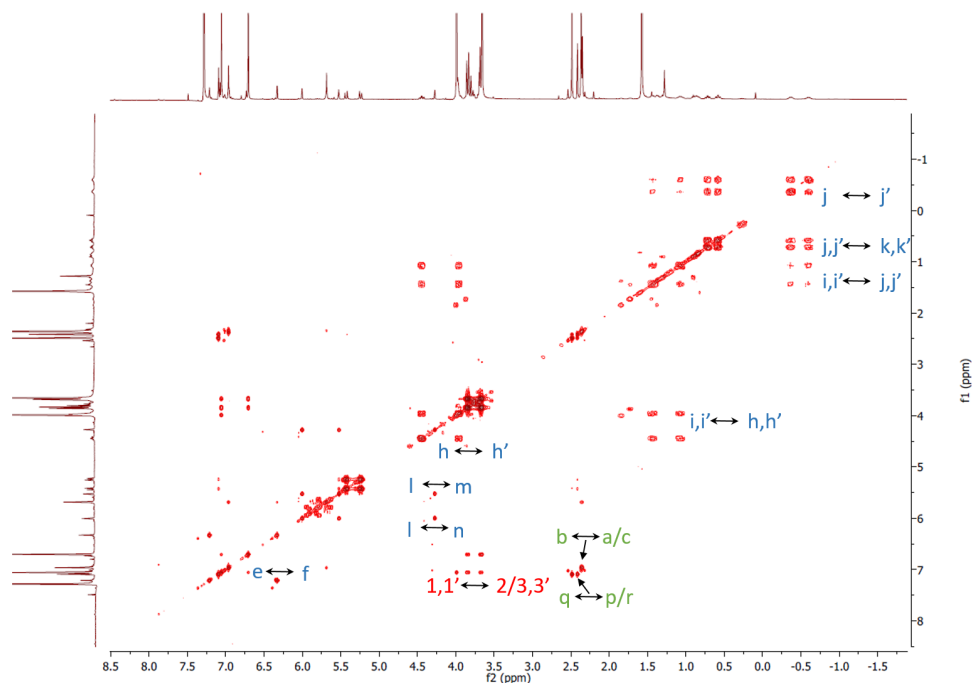


Figure S21. ^1H - ^1H COSY (500 MHz, CHCl_3 , 298 K) spectrum of the [2]rotaxane **3a**.

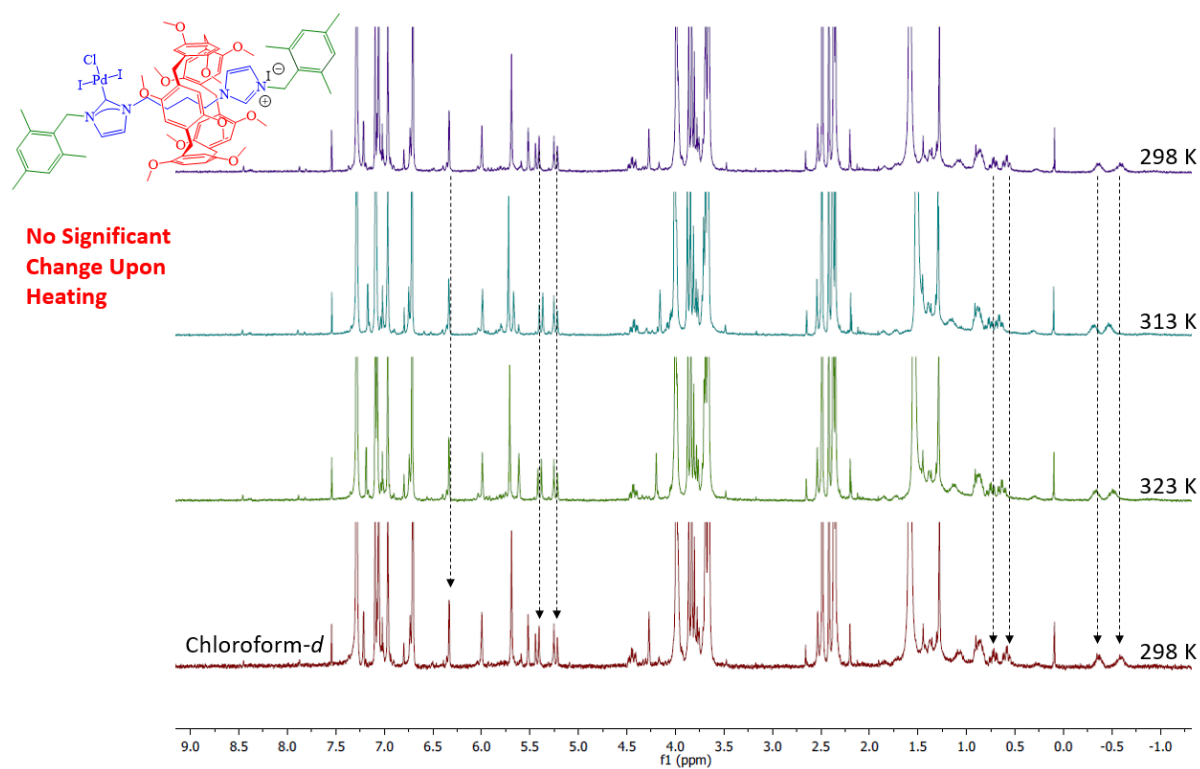


Figure S22. ^1H (400 MHz, CHCl_3 , VT) spectra of the [2]rotaxane **3a**. Showing no change in peak positions.

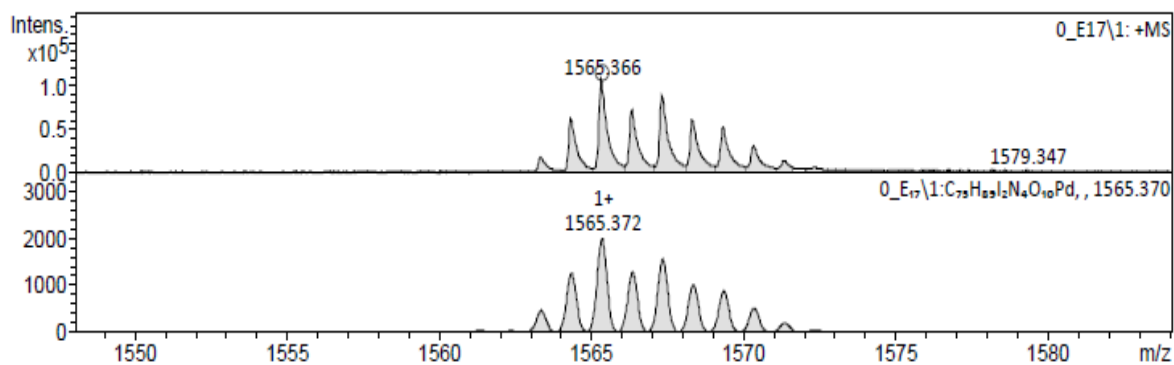


Figure S23. HRMS (MALDI-TOF, positive ionisation mode) of the [2]rotaxane **3a** (top) and calculated for $(\text{C}_{75}\text{H}_{90}\text{N}_4\text{O}_{10})_2\text{Pd}$ bottom.

3b 41% ^1H NMR (400 MHz,) δ 9.17 (dt, $J = 5.0, 1.6$ Hz, 4H), 7.80 (tt, $J = 7.7, 1.6$ Hz, 2H), 7.46 – 7.38 (m, 4H), 7.08 (d, $J = 2.1$ Hz, 2H), 7.02 (s, 4H), 6.94 (s, 10H), 6.30 (d, $J = 2.0$ Hz, 2H), 5.66 (d, 4H), 3.76 (s, 10H), 3.72 (s, 30H), 3.66 – 3.56 (m, 4H), 2.37 (s, 18H), 0.01 – -0.19 (m, 4H), -1.68 – -1.83 (m, 4H) ppm. ^{13}C NMR (101 MHz, Chloroform- d) δ 153.76, 150.98, 143.65, 138.95, 138.74, 137.65, 129.35, 129.15, 127.70, 124.54, 120.95, 118.50, 114.93, 58.38, 50.93, 50.75, 29.14, 27.10, 24.98, 21.16, 20.46.

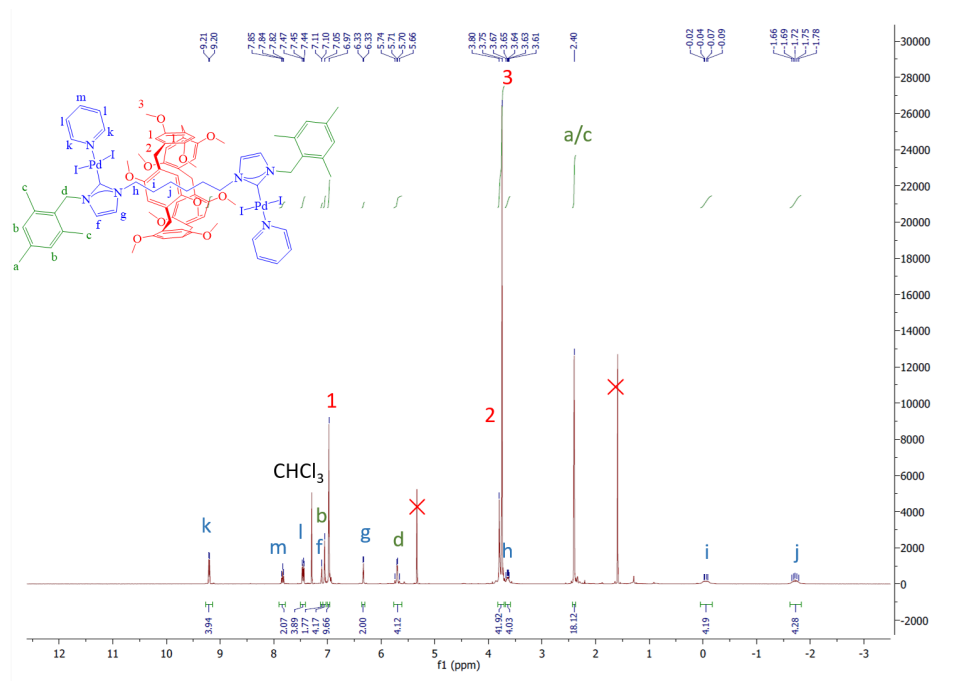


Figure S24. ^1H NMR (400 MHz, CHCl_3 , 298 K) Spectrum of the [2]rotaxane **3b**.

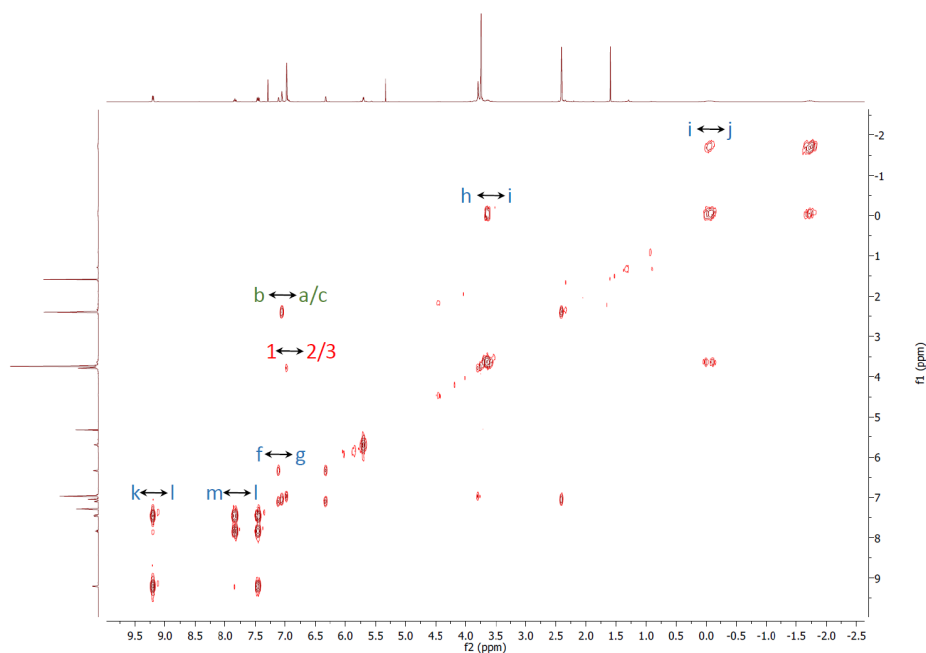


Figure S25. ^1H - ^1H COSY (500 MHz, CHCl_3 , 298 K) spectrum of the [2]rotaxane **3b**.

3c 45% ^1H NMR (400 MHz,) δ 9.15 (dt, $J = 5.0, 1.6$ Hz, 4H), 7.84 (m, 2H), 7.47 – 7.40 (m, 4H), 7.39 (d, $J = 2.1$ Hz, 2H), 7.05 – 6.99 (m, 4H), 6.96 (s, 10H), 6.39 (d, $J = 2.0$ Hz, 2H), 5.62 (s, 4H), 4.15-4.09 (m, 4H), 3.80 (s, 30H), 3.78 (s, 10H), 2.39 (s, 12H), 2.38 (s, 6H), 1.16 – 1.04 (m, 4H), -0.45 (s, 4H), -2.04 (s, 4H) ppm. ^{13}C NMR (101 MHz, Chloroform- d) δ 153.88, 150.78, 138.93, 137.76, 129.41, 128.78, 128.25, 124.59, 119.96, 119.53, 114.46, 114.06, 57.22, 55.80, 52.39, 50.40, 29.66, 29.22, 28.57, 27.09, 26.54, 21.16, 20.55, 1.06.

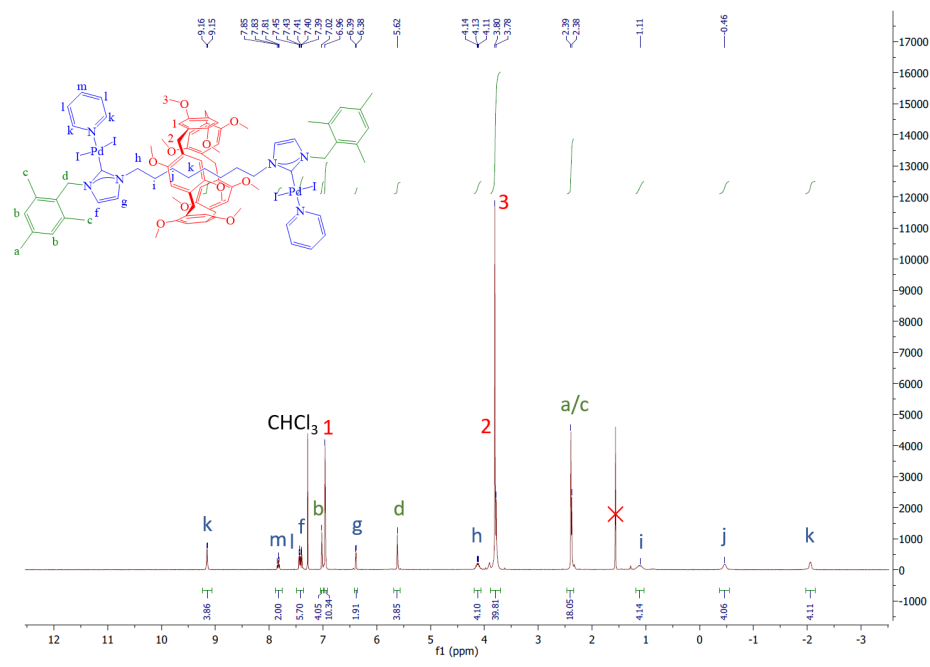


Figure S26. ^1H NMR (400 MHz, CHCl_3 , 298 K) Spectrum of the [2]rotaxane **3c**.

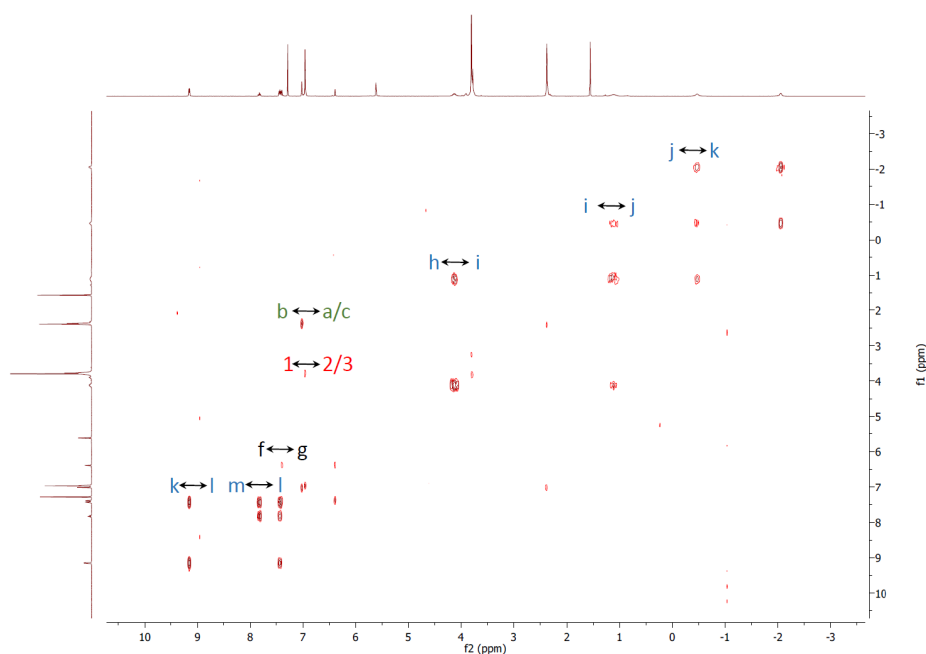


Figure S27. ^1H - ^1H COSY (500 MHz, CHCl_3 , 298 K) spectrum of the [2]rotaxane **3c**.

General procedure for Pd-[2]-Rotaxane **3b**, **3c** and **6a** from **1a-c**.

1a-c (0.0810 mmol) was added to a flame dried flask which had been backfilled with nitrogen three times. Anhydrous pyridine (10 mL) was added via canula, followed by $\text{Pd}(\text{CH}_3\text{CN})_2\text{Cl}_2$ (0.243 mmol), KI (1.215 mmol) and K_2CO_3 (0.486 mmol). The mixture was heated to reflux and stirred overnight under a nitrogen atmosphere and under the exclusion of light. All volatiles were evaporated under reduced pressure and the residue was redissolved in chloroform and water. The organic layer was separated and washed with water, 5% CuSO_4 aq. and brine and subsequently dried over MgSO_4 and

filtered. The solvent was removed under reduced pressure and the residue subjected to a silica pad (CH_2Cl_2) to afford **3b**, **3c** or **6a** as an orange powder.

6a 78% ^1H NMR (400 MHz, Chloroform-*d*) δ 9.14 (dt, $J = 5.0, 1.6$ Hz, 4H), 7.73 (tt, $J = 7.7, 1.6$ Hz, 2H), 7.39 – 7.30 (m, 4H), 6.97 (s, 4H), 6.94 (d, $J = 2.1$ Hz, 2H), 6.29 (d, $J = 2.1$ Hz, 2H), 5.58 (s, 4H), 4.60 (s, 4H), 2.34 (s, 16H), 2.20 (s, 6H) ppm. ^{13}C NMR (101 MHz, CDCl_3) δ 154.01, 144.72, 140.02, 138.91, 137.47, 129.33, 124.48, 109.99, 100.85, 66.39, 51.22, 21.08, 20.46, 19.34.

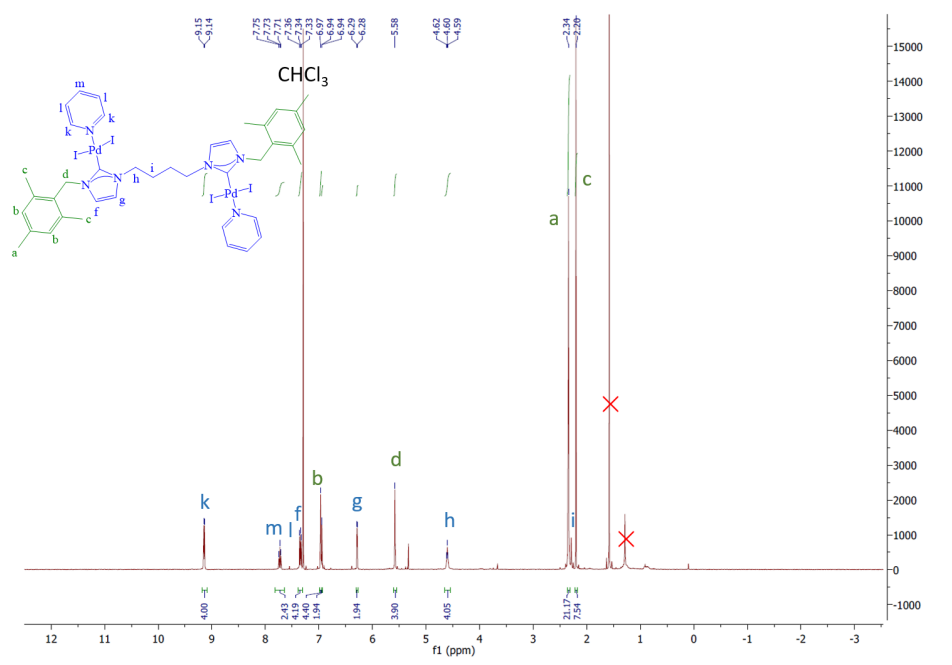


Figure S28. ^1H NMR (400 MHz, CHCl_3 , 298 K) Spectrum of the [2]rotaxane **6a**.

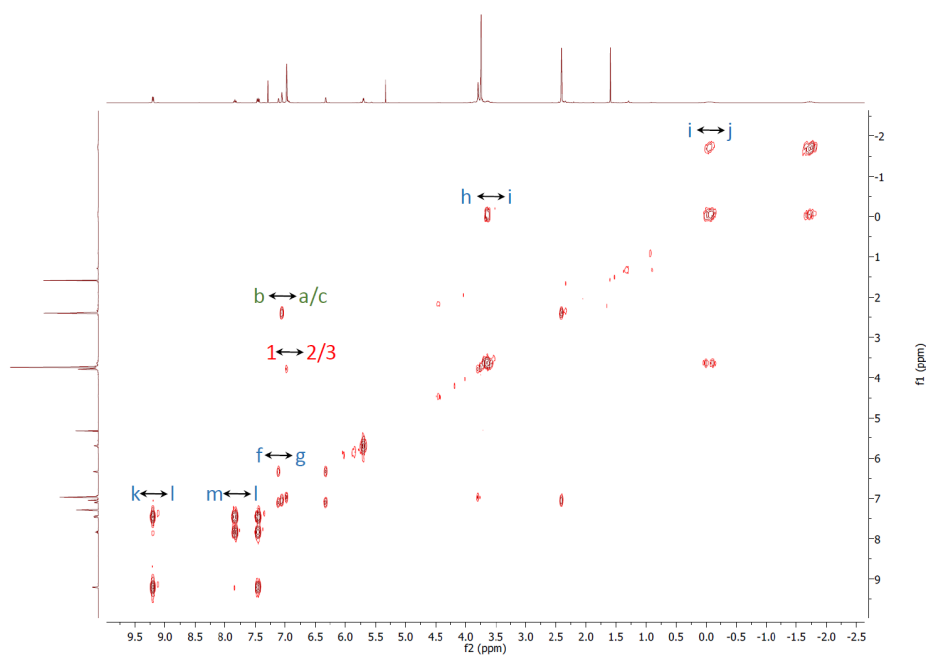
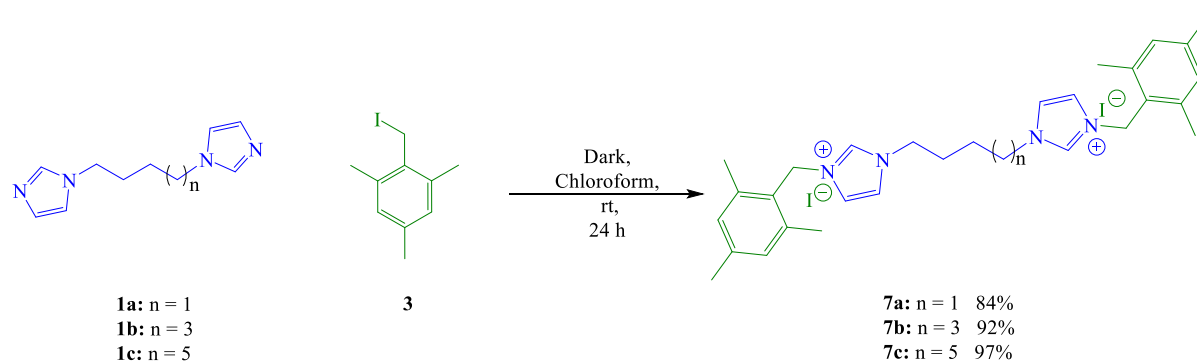


Figure S29. ^1H - ^1H COSY (500 MHz, CHCl_3 , 298 K) spectrum of the [2]rotaxane **6a**.

General procedure for unthreaded stoppered rods 4a-c



Scheme S2. Synthesis of **4(a-c)** with reaction conditions and yields.

Bis imidazole alkane (0.24 mmol) was dissolved in chloroform (10mL) and 2-(iodomethyl)-1,3,5-trimethylbenzene (0.6 mmol) was added under the exclusion of light. The mixture was stirred over night at room temperature. The solvent was removed under reduced pressure and the crude product was purified by silica chromatography (chloroform: methanol 90:10 → 80:20) to give the final products as off-white solids.

4a 84% ^1H NMR (400 MHz, Chloroform-*d*) δ 9.88 (s, 2H), 7.92 (t, J = 1.8 Hz, 2H), 6.93 (s, 4H), 6.81 (s, 2H), 5.51 (s, 4H), 4.58 (s, 4H), 2.30 (s, 22H). ^{13}C NMR (101 MHz, Chloroform-*d*) δ 140.04, 138.17, 135.74, 129.99, 125.07, 123.43, 120.57, 49.35, 48.26, 26.76, 21.07, 20.22. HRMS (ESI+) m/z : 228.1631 ($[\text{M}2^+]$, calc. for $[\text{C}_{30}\text{H}_{40}\text{N}_4]2^+$ = 228.1621).

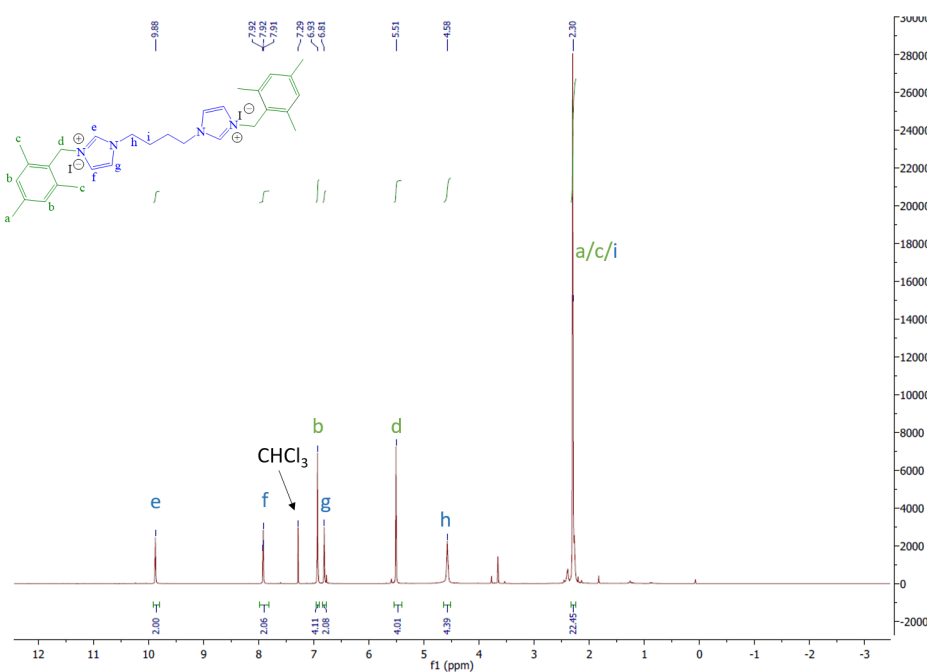


Figure S30. ^1H NMR (400 MHz, CHCl_3 , 298 K) spectrum of the **4a**.

4b 92% ^1H NMR (400 MHz, Chloroform-*d*) δ 10.16 (s, 2H), 7.65 (s, 2H), 6.96 (s, 4H), 6.78 (s, 2H), 5.57 (s, 4H), 4.47 (t, J = 7.4 Hz, 4H), 2.33 (s, 12H), 2.32 (s, 6H), 2.18 – 2.05 (m, 4H), 1.61 (t, J = 6.8 Hz, 4H).

^{13}C NMR (101 MHz, Chloroform-*d*) δ 138.18, 136.24, 130.01, 125.13, 122.74, 120.49, 49.90, 48.20, 29.71, 24.66, 21.07, 20.14. HRMS (ESI+) m/z : 242.1790 ($[\text{M}^2]^+$, calc. for $[\text{C}_{32}\text{H}_{44}\text{N}_4]^2+$ = 242.1778).

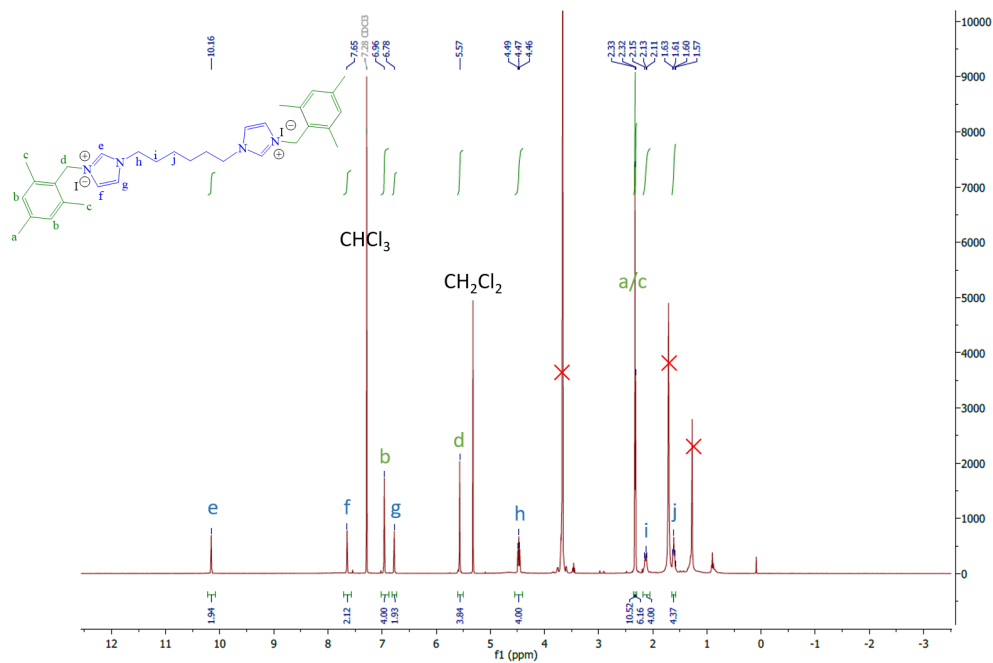


Figure S31. ^1H NMR (400 MHz, CHCl_3 , 298 K) spectrum of **4b**.

4c 97% ^1H NMR (400 MHz, Chloroform-*d*) δ 10.10 (s, 2H), 7.78 (s, 2H), 6.92 (s, 4H), 6.84 (s, 2H), 5.55 (s, 4H), 4.41 (t, J = 7.5 Hz, 4H), 2.29 (s, 18H), 2.00 (s, 4H), 1.42 (s, 8H). ^{13}C NMR (101 MHz, Chloroform-*d*) δ 139.96, 138.09, 135.90, 129.97, 125.23, 123.10, 120.58, 50.14, 48.05, 29.71, 27.73, 25.32, 21.07, 20.11. HRMS (ESI+) m/z : 256.1958 ($[\text{M}^2]^+$, calc. for $[\text{C}_{34}\text{H}_{48}\text{N}_4]^2+$ = 256.1934).

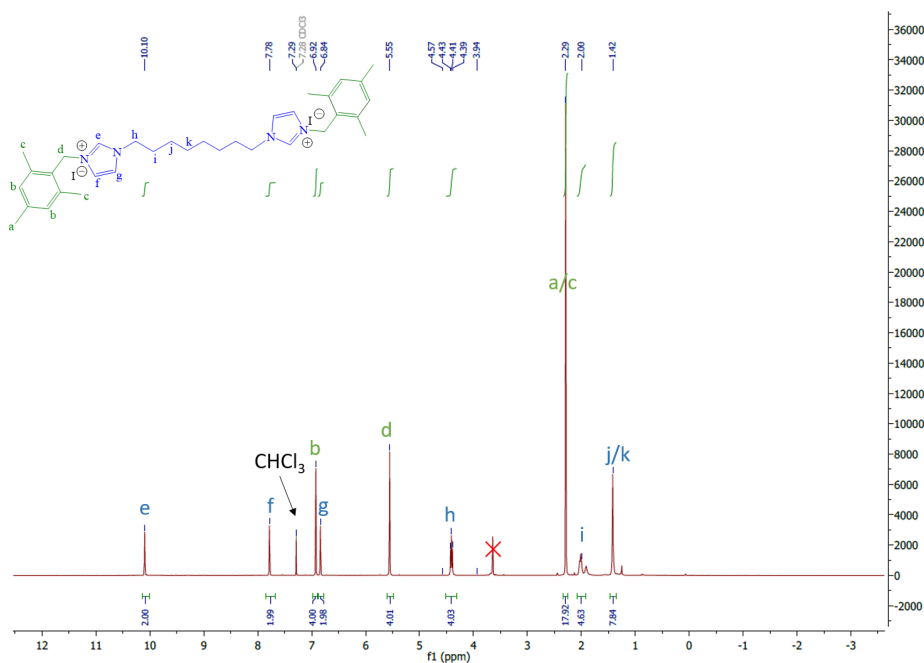
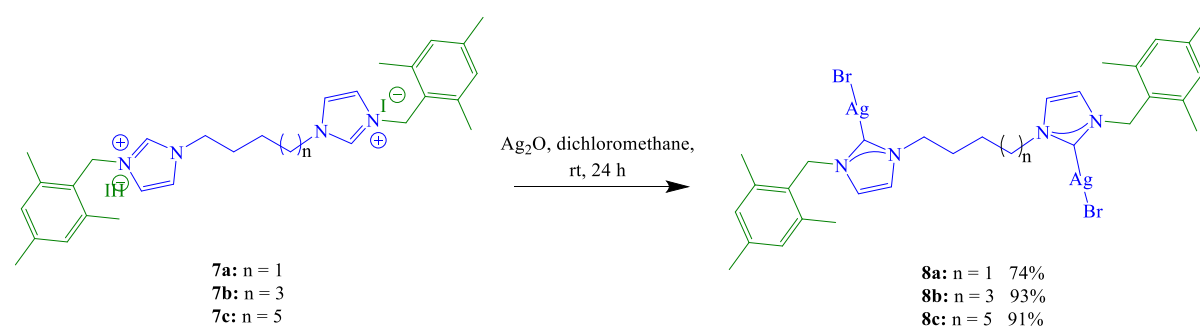


Figure S32. ^1H NMR (400 MHz, CHCl_3 , 298 K) spectrum of **4c**.

General procedure for silver(I) coordination to unthreaded stoppered rods 5a-c



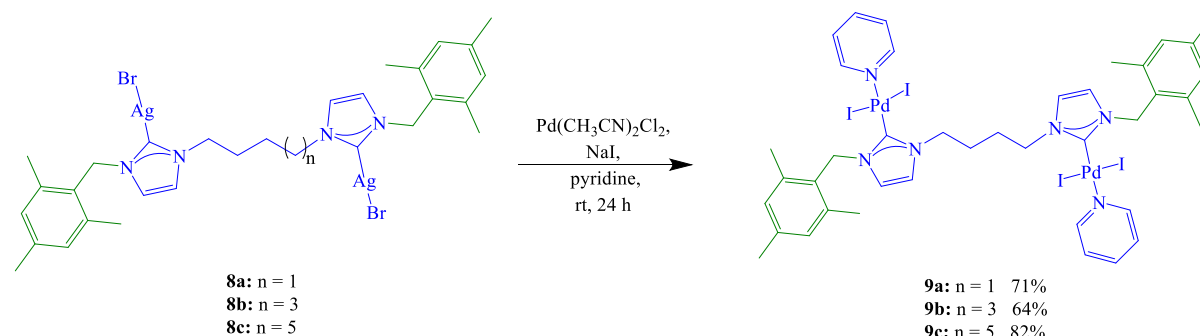
To solution of **4a-c** (0.275 mmol) in CH₂Cl₂ (25 mL) was added Ag₂O (0.550 mmol) and the mixture was stirred at room temperature overnight under the exclusion of light. The mixture was filtered through a celite plug and the organic fractions were combined, dried over anhydrous MgSO₄ and the solvent removed under reduced pressure to afford the crude product as an off white powder. This was redissolved in CH₂Cl₂ (1mL) and added dropwise to cold hexane (20 mL). The white precipitate was collected by filtration under reduced pressure, washed with hexane and dried to afford **5a-c** as white solids.

5a 74% ¹H NMR (400 MHz, Chloroform-*d*) δ 7.05 (d, *J* = 1.5 Hz, 2H), 6.91 (s, 4H), 6.59 – 6.54 (m, 2H), 5.29 (s, 4H), 4.18 (s, 4H), 2.29 (s, 6H), 2.24 (s, 12H), 1.89 (s, 4H). ¹³C NMR (101 MHz, Chloroform-*d*) δ 139.03, 137.77, 129.73, 127.58, 120.88, 120.31, 70.53, 51.36, 49.74, 28.36, 21.04, 20.03.

5b 93% ¹H NMR (400 MHz, Chloroform-*d*) δ 7.07 (d, *J* = 1.6 Hz, 2H), 6.91 (s, 4H), 6.56 (d, *J* = 1.5 Hz, 2H), 5.28 (s, 4H), 4.13 (t, *J* = 7.0 Hz, 4H), 2.28 (s, 6H), 2.25 (s, 12H), 1.86 – 1.78 (m, 4H), 1.45 – 1.36 (m, 4H). ¹³C NMR (101 MHz, Chloroform-*d*) δ 138.98, 137.75, 129.71, 127.70, 121.02, 120.02, 53.49, 51.53, 49.62, 31.25, 25.28, 21.03, 20.00.

5c 91% ¹H NMR (400 MHz, Chloroform-*d*) δ 7.00 (d, *J* = 1.5 Hz, 2H), 6.92 (s, 4H), 6.57 (s, 2H), 5.27 (s, 4H), 4.10 (t, *J* = 7.2 Hz, 4H), 2.29 (s, 6H), 2.25 (s, 12H), 1.82 (p, *J* = 6.6, 6.2 Hz, 4H), 1.41 – 1.29 (m, 8H). ¹³C NMR (101 MHz, Chloroform-*d*) δ 139.00, 137.77, 129.71, 127.66, 120.76, 119.98, 51.92, 49.65, 31.17, 28.46, 25.91, 21.03, 19.99.

General procedure for palladium (II) coordination to unthreaded stoppered rods 6a-c



5a-c (0.240mmol) was added to a flame dried flask which had been backfilled with nitrogen three times. Anhydrous pyridine (10 mL) was added via canula, followed by Pd(CH₃CN)₂Cl₂ (0.577mmol) and KI (1.15mmol). The mixture was heated to reflux and stirred overnight under a nitrogen atmosphere and under the exclusion of light. All volatiles were evaporated under reduced pressure

and the residue was redissolved in chloroform and water. The organic layer was separated and washed with water, 5% CuSO₄ aq. and brine and subsequently dried over MgSO₄ and filtered. The solvent was removed under reduced pressure and the residue subjected to a silica pad (CH₂Cl₂) to afford **6a-c** as orange powders.

6a 71% ¹H and ¹³C NMR in conjunction with spectra discussed above.

6b 64% ¹H NMR (400 MHz, Chloroform-*d*) δ 9.10 (d, *J* = 5.7 Hz, 4H), 7.72 (t, *J* = 8.4 Hz, 2H), 7.34 (d, *J* = 6.1 Hz, 4H), 6.96 (s, 4H), 6.89 (s, 2H), 6.24 (s, 2H), 5.56 (s, 4H), 4.50 – 4.40 (m, 4H), 2.33 (s, 18H), 2.22 – 2.14 (m, 4H), 1.64 (s, 4H). ¹³C NMR (101 MHz, Chloroform-*d*) δ 153.88, 153.02, 138.87, 138.73, 137.68, 129.36, 127.38, 124.56, 121.01, 120.07, 51.70, 50.47, 29.16, 26.15, 21.20, 20.52.

6c 82% ¹H NMR (400 MHz, Chloroform-*d*) δ 9.10 (d, *J* = 4.9 Hz, 4H), 7.74 (t, *J* = 7.7 Hz, 2H), 7.35 (d, *J* = 7.6 Hz, 4H), 6.96 (s, 4H), 6.85 (d, *J* = 2.1 Hz, 2H), 6.25 (d, *J* = 2.0 Hz, 2H), 5.56 (s, 4H), 4.45 – 4.37 (m, 4H), 2.33 (s, 18H), 2.10 (s, 4H), 1.51 (s, 8H). ¹³C NMR (101 MHz, Chloroform-*d*) δ 153.90, 153.04, 144.18, 138.88, 138.72, 137.68, 129.34, 127.39, 124.52, 120.85, 120.01, 51.86, 50.46, 29.42, 28.90, 26.58, 21.17, 20.50.

NMR Spectra Comparisons

Rod versus Rotaxane ¹H NMR shift comparisons.

$$\text{Shielding} = \text{Rod Chemical Shift (ppm)} - \text{Rotaxane Chemical Shift (ppm)}$$

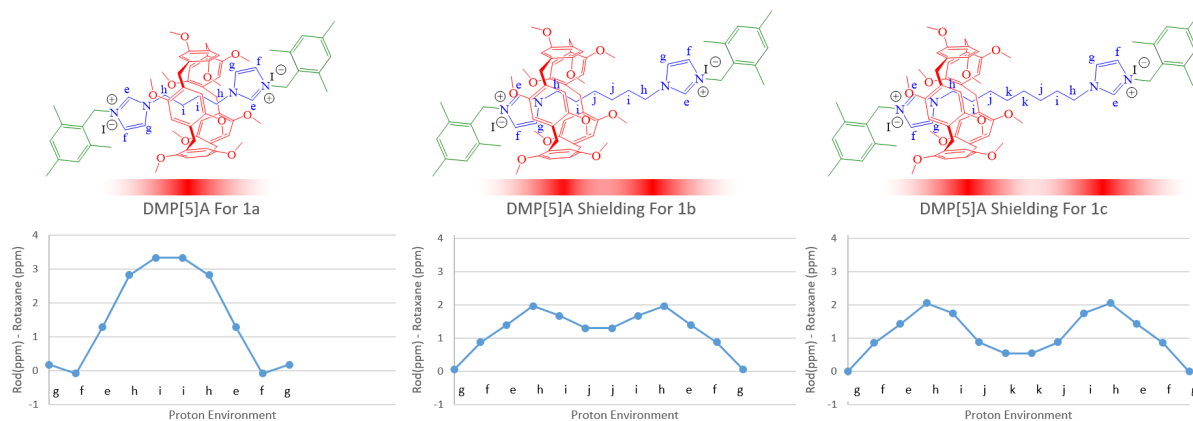


Figure S33. Position of the pillararene along the rod in [2]rotaxanes **1a-c**. Rod (ppm) – Rotaxane (ppm).

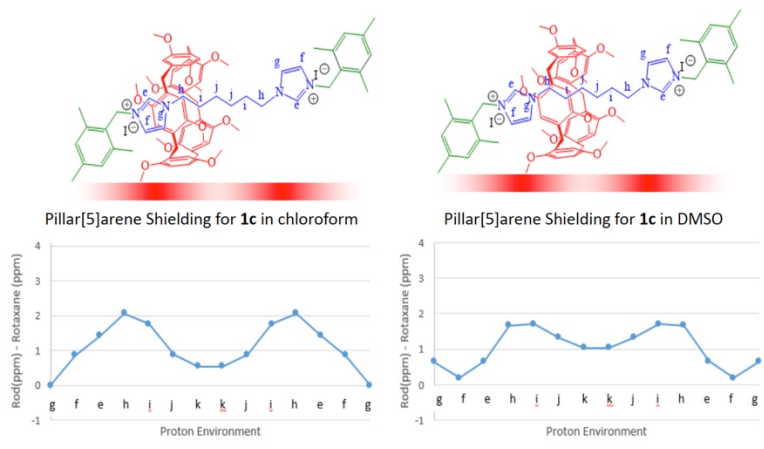


Figure S34. Position of the pillararene along the rod in [2]rotaxanes **1c** in Chloroform (left) and DMSO (right). Rod (ppm) – Rotaxane (ppm).

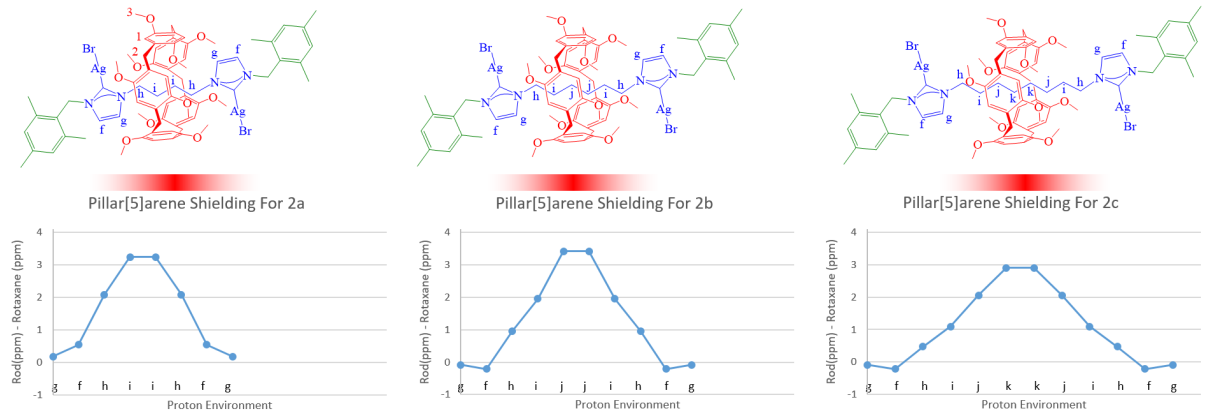


Figure S35. Position of the pillararene along the rod in [2]rotaxanes **2a-c**. Rod (ppm) – Rotaxane (ppm).

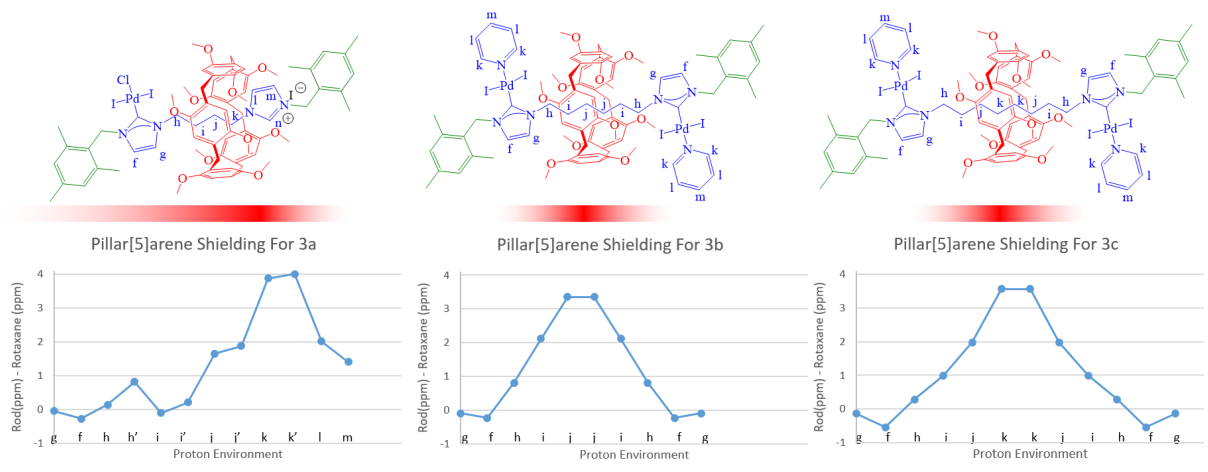


Figure S36. Position of the pillararene along the rod in [2]rotaxanes **3a-c**. Rod (ppm) – Rotaxane (ppm).

Series 6a, 1a, 2a

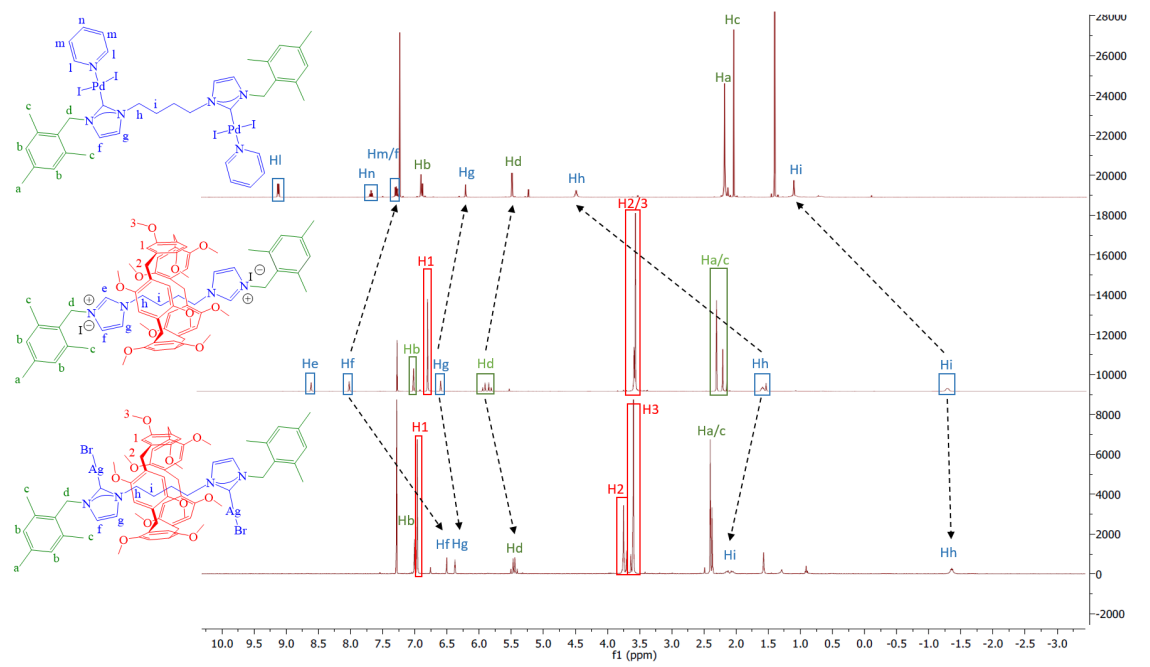


Figure S37. Schematic illustration showing the NMR shifts due dethreading of **1a** to form **6a** and the confinement of pillar[5]arene by the coordination of silver (I) in **2a**.

Series a

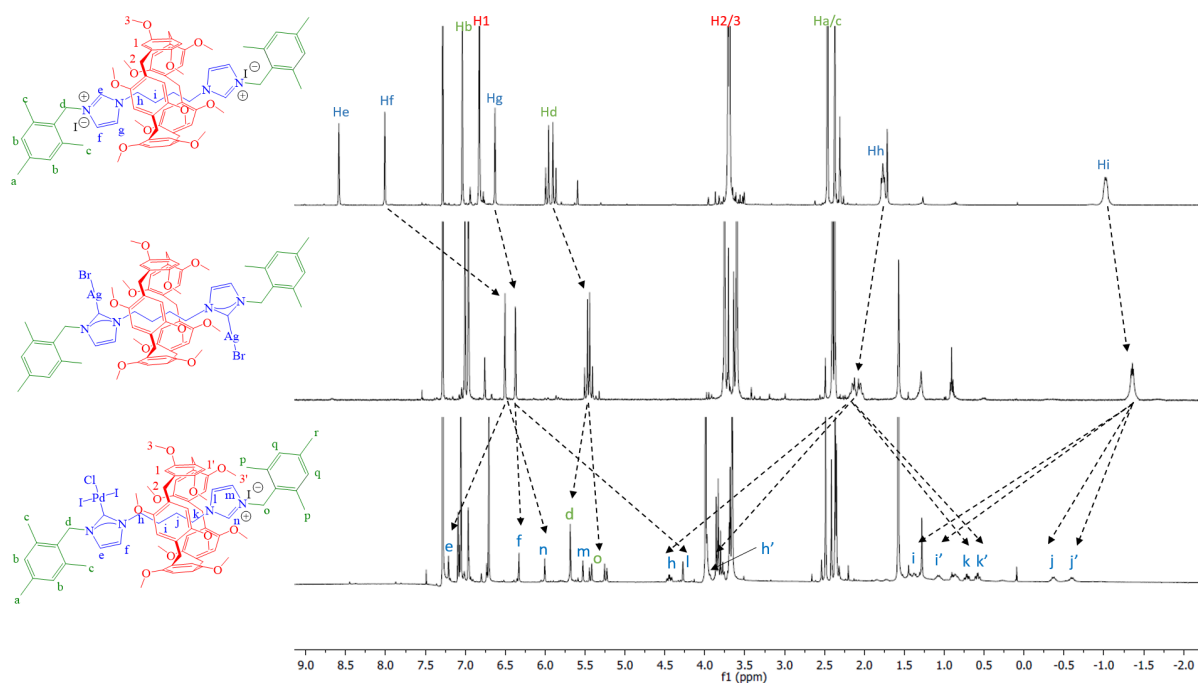


Figure S38. Schematic illustration showing the NMR shifts of **1a** upon Ag(I) coordination **2a** and subsequent palladium(II) coordination **3a**.

Series b

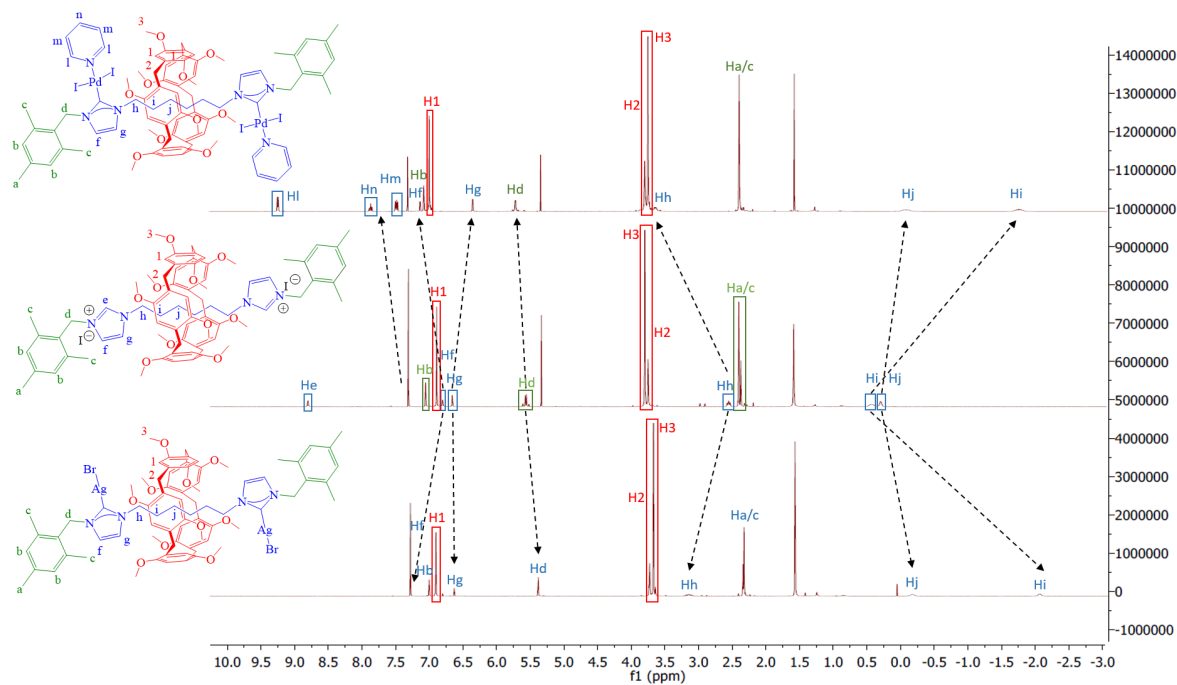


Figure S39. Schematic illustration showing the NMR shifts due to the confinement of pillar[5]arene by the coordination of palladium (II) **3b** and silver (I) **2b**.

Series c

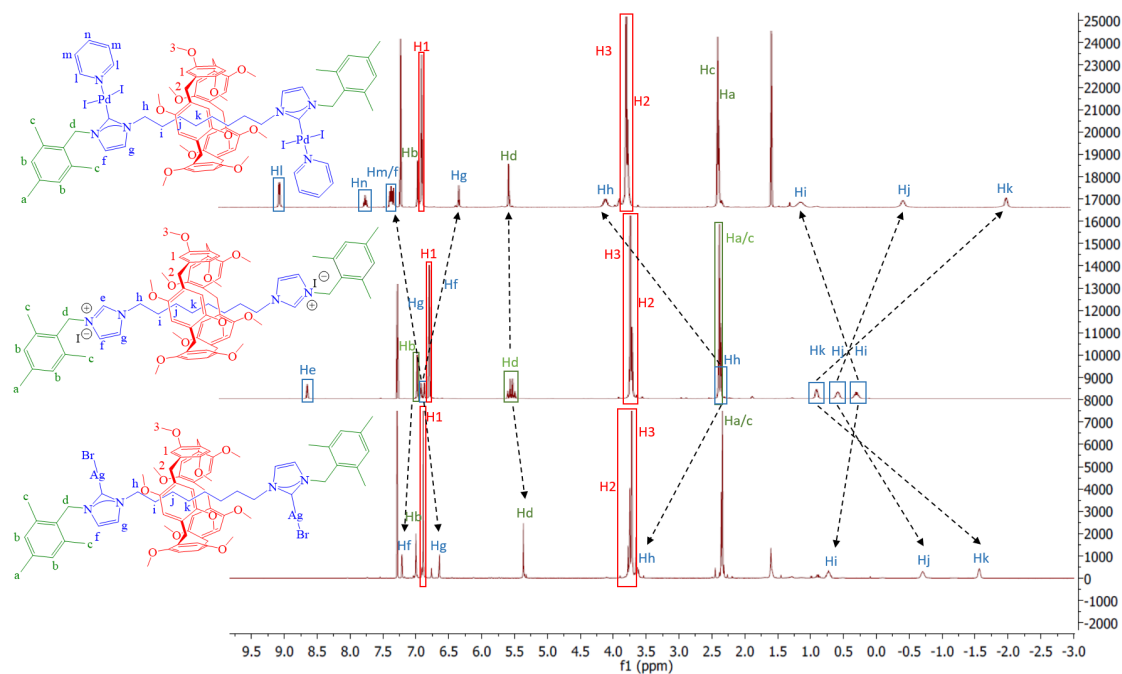


Figure S40. Schematic illustration showing the NMR shifts due to the confinement of pillar[5]arene by the coordination of palladium (II) **3c** and silver (I) **2c**.

Ag Protodemetalation with TFA

[2]rotaxane (**2a-c**) was dissolved in chloroform and TFA was added dropwise. A white precipitate formed which was removed by filtration. The filtrate was dried under reduced pressure to yield [2]rotaxane (**1a-c**).

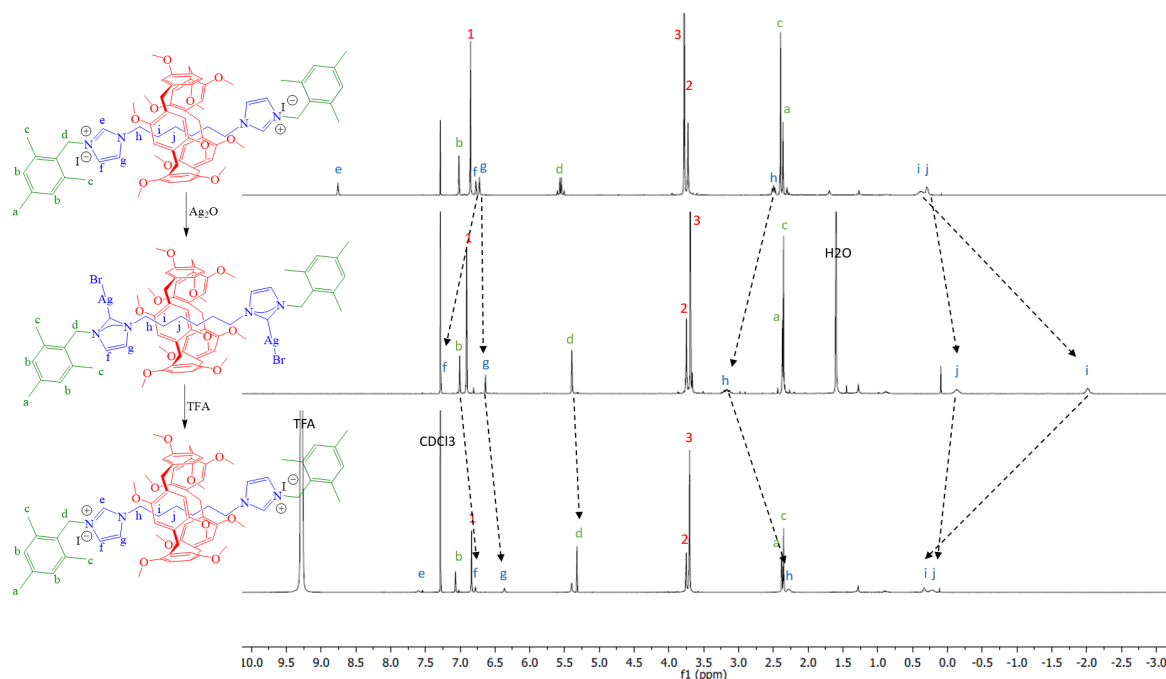


Figure S41. ^1H NMR of **2b** before and after (**1b**) Ag protodemetalation with TFA.

Crystallographic Details

Experimental

Single crystals were selected and mounted using fomblin film on a micromount. Data was collected with a SuperNova, Atlas S2 diffractometer for **1a**, **1b**, **2a Cl**, **2c**, **3a**, **3b** and **3c**, and a XtaLAB PRO MM007, PILATUS3 R 200K diffractometer for **1c**, **2a Br** and **2b**. The crystals were kept at 120(2) K during data collection. Using Olex2 [1], the structures were solved with the ShelXT [2] structure solution program using Intrinsic Phasing and refined with the ShelXL [3] refinement package using Least Squares minimisation.

1a

$\text{C}_{78}\text{H}_{93}\text{Br}_{0.72}\text{Cl}_{10.2775}\text{N}_4\text{O}_{10}$ ($M = 1668.43$ g/mol): monoclinic, space group $C2/c$ (no. 15), $a = 49.652(3)$ Å, $b = 12.0617(4)$ Å, $c = 27.909(2)$ Å, $\beta = 102.619(6)^\circ$, $V = 16310.8(16)$ Å³, $Z = 8$, $T = 120(2)$ K, $\mu(\text{CuK}\alpha) = 4.092$ mm⁻¹, $D_{\text{calc}} = 1.359$ g/cm³, 50074 reflections measured ($6.716^\circ \leq 2\theta \leq 130.176^\circ$), 13868 unique ($R_{\text{int}} = 0.1578$, $R_{\text{sigma}} = 0.1099$) which were used in all calculations. The final R_1 was 0.0963 ($I > 2\sigma(I)$) and wR_2 was 0.2799 (all data). GoF = 1.291.

1b

$\text{C}_{79}\text{H}_{98}\text{Cl}_{412}\text{N}_4\text{O}_{10}$ ($M = 1659.21$ g/mol): monoclinic, space group $P2_1/c$ (no. 14), $a = 20.0828(3)$ Å, $b = 12.8444(2)$ Å, $c = 31.5223(5)$ Å, $\beta = 102.9695(15)^\circ$, $V = 7923.8(2)$ Å³, $Z = 4$, $T = 120(2)$ K, $\mu(\text{CuK}\alpha) = 7.939$ mm⁻¹, $D_{\text{calc}} = 1.391$ g/cm³, 95903 reflections measured ($7.46^\circ \leq 2\theta \leq 133.198^\circ$), 14000 unique

($R_{\text{int}} = 0.0850$, $R_{\text{sigma}} = 0.0356$) which were used in all calculations. The final R_1 was 0.1494 ($I > 2\sigma(I)$) and wR_2 was 0.3340 (all data). GoF = 1.085.

1c

$\text{C}_{81}\text{H}_{98}\text{Cl}_3\text{I}_2\text{N}_4\text{O}_{10}$ ($M = 1647.78$ g/mol): monoclinic, space group $P2_1$ (no. 4), $a = 16.3045(5)$ Å, $b = 12.8881(3)$ Å, $c = 20.4913(5)$ Å, $\beta = 107.067(3)^\circ$, $V = 4116.31(19)$ Å³, $Z = 2$, $T = 120(2)$ K, $\mu(\text{CuK}\alpha) = 7.346$ mm⁻¹, $D_{\text{calc}} = 1.329$ g/cm³, 55391 reflections measured ($8.212^\circ \leq 2\theta \leq 133.178^\circ$), 14052 unique ($R_{\text{int}} = 0.3012$, $R_{\text{sigma}} = 0.1382$) which were used in all calculations. The final R_1 was 0.1536 ($I > 2\sigma(I)$) and wR_2 was 0.4041 (all data). GoF = 1.535.

Disordered counterion iodine and solvent chloroform could not be sensibly and the structure was processed using PLATON SQUEEZE [4], which gave an estimate of 424 e- per cell, corresponding to one iodine ion and three chloroform molecules per cell. These molecules were included in the sum formula and calculation of derived parameters.

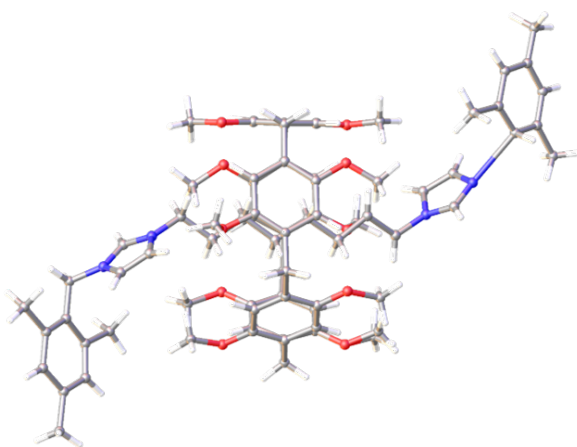


Figure S42. Crystal structure of **1c**. Carbon atoms = grey, oxygen atoms = red, and nitrogen atoms = blue.

2a Br

$\text{C}_{77}\text{H}_{90}\text{Ag}_2\text{Br}_2\text{Cl}_6\text{N}_4\text{O}_{10}$ ($M = 1819.78$ g/mol): triclinic, space group P-1 (no. 2), $a = 12.5204(10)$ Å, $b = 16.9379(8)$ Å, $c = 19.2586(7)$ Å, $\alpha = 77.409(4)^\circ$, $\beta = 80.515(5)^\circ$, $\gamma = 80.739(5)^\circ$, $V = 3898.2(4)$ Å³, $Z = 2$, $T = 120(2)$ K, $\mu(\text{CuK}\alpha) = 7.601$ mm⁻¹, $D_{\text{calc}} = 1.550$ g/cm³, 53950 reflections measured ($7.22^\circ \leq 2\theta \leq 163.492^\circ$), 15508 unique ($R_{\text{int}} = 0.2027$, $R_{\text{sigma}} = 0.1838$) which were used in all calculations. The final R_1 was 0.0860 ($I > 2\sigma(I)$) and wR_2 was 0.2767 (all data). GoF = 1.055.

2a Cl

$\text{C}_{77}\text{H}_{90}\text{Ag}_2\text{Cl}_8\text{N}_4\text{O}_{10}$ ($M = 1730.86$ g/mol): triclinic, space group P-1 (no. 2), $a = 12.4582(3)$ Å, $b = 16.8795(4)$ Å, $c = 19.1895(5)$ Å, $\alpha = 77.554(2)^\circ$, $\beta = 80.633(2)^\circ$, $\gamma = 80.930(2)^\circ$, $V = 3856.37(17)$ Å³, $Z = 2$, $T = 120(2)$ K, $\mu(\text{CuK}\alpha) = 7.107$ mm⁻¹, $D_{\text{calc}} = 1.491$ g/cm³, 42843 reflections measured ($4.758^\circ \leq 2\theta \leq 133.194^\circ$), 13599 unique ($R_{\text{int}} = 0.0400$, $R_{\text{sigma}} = 0.0355$) which were used in all calculations. The final R_1 was 0.0547 ($I > 2\sigma(I)$) and wR_2 was 0.1774 (all data). GoF = 1.354.

2b

$C_{81}H_{93}Ag_2Br_2Cl_{12}N_4O_{10}$ ($M = 2083.55$ g/mol): monoclinic, space group $P2_1$ (no. 4), $a = 12.1948(5)$ Å, $b = 28.7424(6)$ Å, $c = 12.6578(4)$ Å, $\beta = 101.327(4)^\circ$, $V = 4350.2(3)$ Å³, $Z = 2$, $T = 120(2)$ K, $\mu(\text{CuK}\alpha) = 8.549$ mm⁻¹, $D_{\text{calc}} = 1.591$ g/cm³, 20543 reflections measured ($7.394^\circ \leq 2\theta \leq 153.392^\circ$), 11419 unique ($R_{\text{int}} = 0.0668$, $R_{\text{sigma}} = 0.0709$) which were used in all calculations. The final R_1 was 0.0986 ($I > 2\sigma(I)$) and wR_2 was 0.3002 (all data). GoF = 1.139.

Disordered solvent chloroform molecules could not be sensibly modelled and the structure was processed using PLATON SQUEEZE [4], which gave an estimate of 136 e- per cell, corresponding to two chloroform molecules per cell. These molecules were included in the sum formula and calculation of derived parameters.

2c

$C_{81}H_{98}Ag_2BrCl_7N_4O_{10}$ ($M = 1831.43$ g/mol): monoclinic, space group $P2_1$ (no. 4), $a = 16.4695(4)$ Å, $b = 12.8394(4)$ Å, $c = 20.6024(6)$ Å, $\beta = 107.615(3)^\circ$, $V = 4152.3(2)$ Å³, $Z = 2$, $T = 120(2)$ K, $\mu(\text{CuK}\alpha) = 6.886$ mm⁻¹, $D_{\text{calc}} = 1.465$ g/cm³, 18124 reflections measured ($5.63^\circ \leq 2\theta \leq 147.426^\circ$), 10970 unique ($R_{\text{int}} = 0.0684$, $R_{\text{sigma}} = 0.0652$) which were used in all calculations. The final R_1 was 0.0577 ($I > 2\sigma(I)$) and wR_2 was 0.1452 (all data). GoF = 0.974.

The crystal collected was a 2-component twin. The orientations of the two twin components were determined in CrysAlisPro [5], and integrated to provide a single component HKL file which was used for the initial solution, and a multi-component HKL file which was used for subsequent structure refinement.

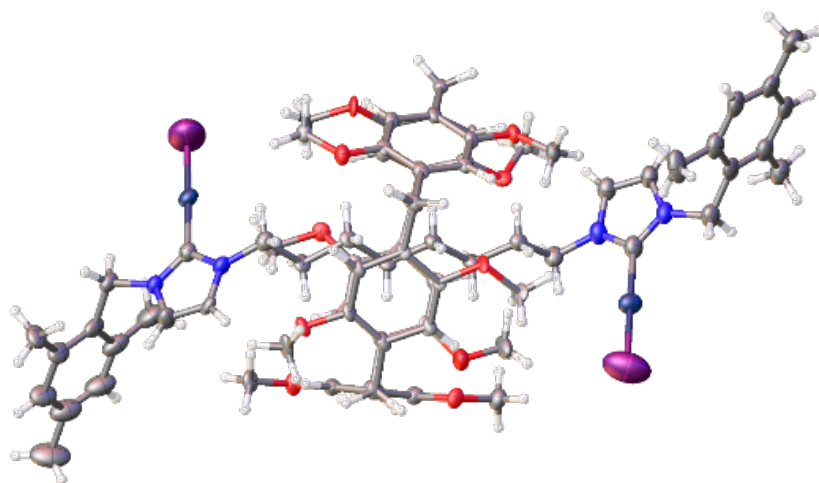


Figure S43. Crystal structure of **2c**. Carbon atoms = grey, oxygen atoms = red, nitrogen atoms = blue, iodine = purple and silver = dark blue.

3a

$C_{79.25}H_{93.25}Cl_{13.84}I_{1.91}N_4O_{10}Pd$ ($M = 2101.46$ g/mol): monoclinic, space group $P2_1/n$ (no. 14), $a = 16.515(2)$ Å, $b = 22.093(3)$ Å, $c = 24.313(2)$ Å, $\beta = 92.023(10)^\circ$, $V = 8952.2(18)$ Å³, $Z = 4$, $T = 120(2)$ K, $\mu(\text{CuK}\alpha) = 11.106$ mm⁻¹, $D_{\text{calc}} = 1.559$ g/cm³, 25705 reflections measured ($5.378^\circ \leq 2\theta \leq 133.202^\circ$), 14455 unique ($R_{\text{int}} = 0.2595$, $R_{\text{sigma}} = 0.3588$) which were used in all calculations. The final R_1 was 0.2550 ($I > 2\sigma(I)$) and wR_2 was 0.6260 (all data). GoF = 0.930.

Equivalent bond lengths and angle of the organic portion of the structure were restrained to be approximately equal. Five- and six-membered rings were constrained to idealised geometries, and restrained to be coplanar with their flanking atoms. Enhanced rigid bond and similarity restraints were applied to the thermal parameters of all non-hydrogen atoms.

The halogen sites coordinated to the palladium atom are statistically disordered between iodide and chloride. The occupancy of each site was refined competitively, converging to iodide:chloride ratios of 0.27:0.73, 0.78:0.22 and 0.86:0.14, for the axial and two equatorial sites respectively. The major component was set to that of the most highly occupied atom at each site, corresponding to two equatorial iodides and an axial chloride, however it is possible that all six arrangements of iodide and chloride are present in the crystal. Pd-Cl distances and Pd-I distances were separately restrained to be approximately equal.

Hydrogen atoms were placed in calculated positions and refined with a riding model. Methyl groups, in general, were refined with a fixed orientation, determined by adjacent groups. For carbon atoms C13B, C36B and C90A, it was necessary to refine as rigid rotors, to prevent close H..H inter- and intra-molecular interactions. For C13B and C90A it was necessary to add H..H relative distance restraints to stabilise the rotation position of the group during refinement.

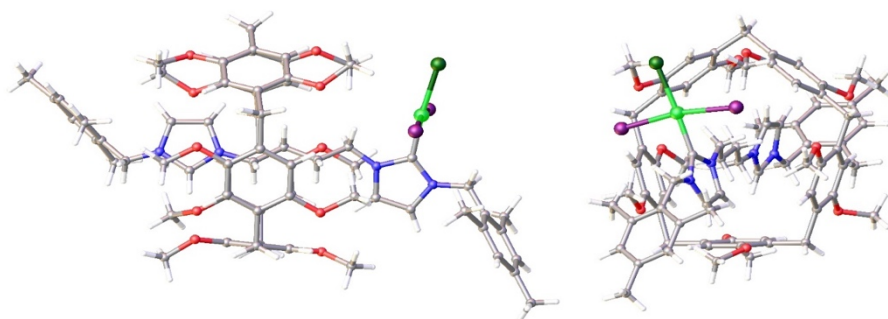


Figure S44. Crystal structure of **3a**. Carbon atoms = grey, oxygen atoms = red, nitrogen atoms = blue, iodine = purple and palladium = green.

3b

$C_{87}H_{102}I_4N_6O_{10}Pd_2$ ($M = 2112.14$ g/mol): monoclinic, space group $P2_1$ (no. 4), $a = 16.2495(7)$ Å, $b = 12.2253(6)$ Å, $c = 21.1205(7)$ Å, $\beta = 92.453(4)^\circ$, $V = 4191.8(3)$ Å³, $Z = 2$, $T = 120(2)$ K, $\mu(\text{CuK}\alpha) = 15.514$ mm⁻¹, $D_{\text{calc}} = 1.673$ g/cm³, 17866 reflections measured ($6.726^\circ \leq 2\theta \leq 148.888^\circ$), 12242 unique ($R_{\text{int}} = 0.0518$, $R_{\text{sigma}} = 0.0416$) which were used in all calculations. The final R_1 was 0.0666 ($I > 2\sigma(I)$) and wR_2 was 0.2143 (all data). GoF = 0.995.

The crystal collected was a 2-component twin. The orientations of the two twin components were determined in CrysAlisPro [5] and integrated to provide a single component HKL file which was used for the final refinement of the structure.

3c

$C_{89}H_{106}I_4N_6O_{10}Pd_2$ ($M = 2140.19$ g/mol): monoclinic, space group $P2_1/c$ (no. 14), $a = 20.0957(6)$ Å, $b = 12.1538(3)$ Å, $c = 37.0911(11)$ Å, $\beta = 103.157(3)^\circ$, $V = 8821.3(4)$ Å³, $Z = 4$, $T = 120(2)$ K, $\mu(\text{MoK}\alpha) = 1.867$ mm⁻¹, $D_{\text{calc}} = 1.612$ g/cm³, 542213 reflections measured ($5.798^\circ \leq 2\theta \leq 57.81^\circ$), 22446 unique

($R_{\text{int}} = 0.2245$, $R_{\text{sigma}} = 0.0927$) which were used in all calculations. The final R_1 was 0.1116 ($I > 2\sigma(I)$) and wR_2 was 0.3418 (all data). GoF = 1.049.

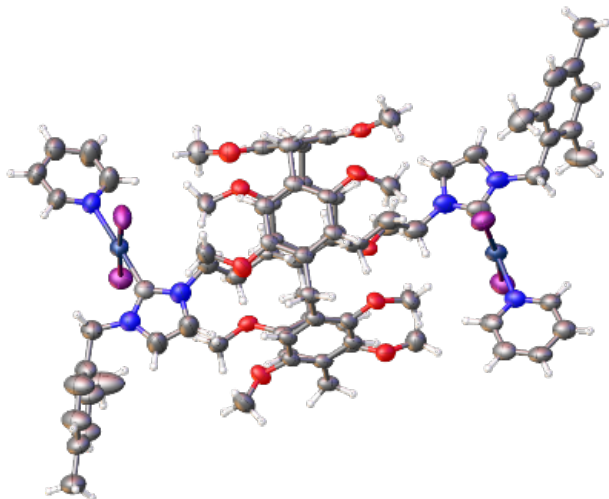


Figure S45. Crystal structure of **3c**. Carbon atoms = grey, oxygen atoms = red, nitrogen atoms = blue, iodine = purple and palladium = green.

References

1. Dolomanov, O.V., Bourhis, L.J., Gildea, R.J, Howard, J.A.K. & Puschmann, H. (2009), *J. Appl. Cryst.* 42, 339-341.
2. Sheldrick, G.M. (2015). *Acta Cryst.* A71, 3-8.
3. Sheldrick, G.M. (2015). *Acta Cryst.* C71, 3-8.
4. Spek, A.L. (2009). *Acta Cryst.* D65, 148-155.
5. Agilent (2014). *CrysAlis PRO*. Agilent Technologies Ltd, Yarnton, Oxfordshire, England.